



**Universidad de Valladolid**



**ESCUELA DE INGENIERÍAS  
INDUSTRIALES**

**UNIVERSIDAD DE VALLADOLID**

**ESCUELA DE INGENIERIAS INDUSTRIALES**

**Grado en Ingeniería Mecánica**

# **ANÁLISIS DEL RENDIMIENTO DE UNA TURBINA EÓLICA MARINA FLOTANTE**

**Autor:**

**Mediavilla Tejeda, Samuel**

**Responsable de Intercambio en la Uva:**

**Eusebio de la Fuente López**

**Universidad de destino:**

**Politécnico di Bari**

Valladolid, mes y año.

TFG REALIZADO EN PROGRAMA DE INTERCAMBIO

---

TÍTULO: Analysis of the performance of a floating offshore wind turbine  
ALUMNO: Samuel Mediavilla Tejeda  
FECHA: 14/01/2025  
CENTRO: Politécnico di Bari  
UNIVERSIDAD: Politécnico di Bari  
TUTOR: Marco Torresi

## RESUMEN

Este TFG analiza el rendimiento de un aerogenerador flotante offshore, específicamente el modelo NREL 5MW OC4 Semisub, instalado en el Mar Adriático, frente a la costa de Bari. Se emplea el software QBlade para modelar y simular el comportamiento de la turbina bajo diferentes condiciones de viento y oleaje.

El trabajo abarca conceptos clave de energía eólica offshore, tipos de turbinas marinas y su interacción con el entorno. Se detallan las propiedades aerodinámicas de las palas a través del método BEM (Blade Element Momentum) para evaluar su rendimiento.

Las simulaciones consideran diversos escenarios climáticos para evaluar la producción de energía y la estabilidad de la estructura. Finalmente, se estima la producción anual de energía (AEP) utilizando la distribución de Weibull, permitiendo analizar la viabilidad del aerogenerador en esta ubicación específica.

## PALABRAS CLAVE

Qblade, Wind Turbine, NREL 5MW Semisub OC4, AEP, BEM Analysis.

## ABSTRACT

This TFG analyzes the performance of a floating offshore wind turbine, specifically the NREL 5MW OC4 Semisub model, installed in the Adriatic Sea, off the coast of Bari. The QBlade software is used to model and simulate the turbine's behavior under different wind and wave conditions.

The study covers key concepts of offshore wind energy, types of marine wind turbines, and their interaction with the environment. The aerodynamic properties of the blades are analyzed using the BEM (Blade Element Momentum) method to assess their performance.

The simulations consider various climatic scenarios to evaluate energy production and structural stability. Finally, the Annual Energy Production (AEP) is estimated using the Weibull distribution, allowing an assessment of the turbine's feasibility in this specific location.

## KEY WORDS

Qblade, Wind Turbine, NREL 5MW Semisub OC4, AEP, BEM Analysis.

---

# ANALYSIS OF THE PERFORMANCE OF A FLOATING OFFSHORE WIND TURBINE

---



## Content

SUMMARY .....	3
1-CONCEPTS.....	4
1.1-WIND ENERGY .....	4
1.2-WIND TURBINES .....	4
1.2.1-OFFSHORE WIND FARMS.....	6
1.2.2-DIFFERENT TYPES OF OFFSHORE WIND TURBINES .....	6
1.2.3-NREL 5MW OC4 SEMISUB.....	9
1.3 - PRINCIPLES OF WIND TURBINE OPERATION .....	11
1.3.1 - WIND ENERGY GENERATION.....	11
1.3.2 - POWER CALCULATION AND EFFICIENCY .....	12
1.4- CLIMATIC CONDITIONS AT SEA.....	13
1.4.1-OCEAN WINDS .....	13
1.4.2-OCEAN WAVES .....	13
1.4.3-INTERACTION BETWEEN WIND AND WAVES .....	14
1.4.4-CHALLENGES OF THE MARINE ENVIRONMENT: CORROSION AND MAINTENANCE.....	14
2-SIMULATION CODE .....	15
2.1-QBLADE .....	15
2.2- INTRODUCTION TO THE PROGRAM.....	15
2.2.1-AERODYNAMIC PROFILE DESING .....	15
2.2.2-ANALYSIS OF AERODYNAMIC PROFILES .....	17
2.2.3-POLAR EXTRAPOLATION TO 360°.....	22
2.2.4-BLADE DESIGN .....	24
2.2.5- BEM ANALYSIS .....	29
4.2.6- DEFINITION OF THE TURBINE AND ITS STRUCTURE .....	35
4.2.7-SIMULATION.....	37
2.2.8-WAVE GENERATOR .....	39
3-SIMULATIONS .....	41

3.1-EXPLANATION OF DATA CHOICE AND RESULTS .....	42
3.1.1-EXPLANATION OF DATA CHOICE.....	42
3.1.2-RESULTS .....	46
3.2-ANNUAL ENERGY PROCUCTION (AEP) .....	48
6-CONCLUSION.....	55
7-REFERENCES .....	56
8-APPENDICES .....	58

# SUMMARY

One of the primary goals of the energy generation sector is to find the best ways to produce clean energy, that is, with the least possible environmental impact.

This paper discusses how offshore wind turbines play a crucial role in the transition to renewable energy sources due to their high energy generation potential and lower visual and acoustic impact compared to onshore wind turbines.

Thanks to their location in areas with constant and higher-speed winds, offshore wind turbines can generate energy much more efficiently than their onshore counterparts. According to an article from the Argentine Wind Chamber (CEA), the electricity generation of an offshore wind turbine can be between 30% and 50% higher than that of an onshore turbine.

This study is carried out using a model of a floating offshore wind turbine, specifically the NREL 5MW OC4 Semisub, under the assumption that it is installed off the coast of Bari, in the Adriatic Sea. To this end, the simulation program QBlade will be used to demonstrate the high efficiency of this offshore model.

# 1-CONCEPTS

## 1.1-WIND ENERGY

Wind energy is one of the most important and sustainable renewable energy sources in the world. Its generation is based on harnessing the kinetic energy of the wind to produce electricity through turbines. This technology has significantly evolved over the past decades, establishing itself as a key solution in the transition toward a carbon-free energy system.

Among the advantages of wind energy, it is worth highlighting that it is a renewable energy source available in most regions of the planet and does not produce greenhouse gases or pollute the air, during operation.

Thanks to the high technological maturity, modern wind turbines have achieved a high degree of efficiency due to innovations that allow for maximizing energy generation, even when wind conditions are moderate.

Of course, wind energy also has some limitations, such as intermittency, since the production depends on wind availability; the lack of wind can lead to fluctuations in the power supply from wind farms. Another issue with wind turbines is their large size and the impact they have on the landscape and bird populations, as well as the substantial economic investment required for their installation, particularly for offshore wind turbines.

## 1.2-WIND TURBINES

Within wind energy, there are several types of wind turbines; for example, we have vertical-axis or horizontal-axis wind turbines, and we also have onshore (land-based) or offshore (marine-based) wind farms. All of these systems operate based on the same principles despite their differences.

Wind turbines convert the kinetic energy of the wind into electrical energy through the following steps:

1-Wind Capture: The aerodynamic blades rotate when impacted by the wind, causing the rotor to move.



2-Mechanical Conversion: The rotor transfers its rotation to the electrical generator via a shaft.

3-Electricity Generation: The electrical generator converts the mechanical energy into electricity, which can then be transmitted to the grid or store (not easily).

The turbines consist of the following components:

- Rotor: Made up of three long, lightweight blades designed to optimize wind capture.
- Generator: Uses technologies such as permanent magnets or induction to convert mechanical energy into electrical energy.
- Tower: Designed to withstand structural and environmental stresses, with heights that vary depending on the site.
- Control System: Incorporates sensors and software to adjust the blade angles and protect the turbine under extreme conditions.

In the following image (Illustration 1), several wind turbines are shown, where the components described above can be seen.



*Illustration 1-wind turbines*

Additionally, offshore turbines are typically designed to withstand marine conditions, featuring anti-corrosion coatings and anchoring systems for deep waters. Since this study will focus on a floating offshore model, we will delve deeper into offshore wind farms, specifically concentrating on the NREL 5MW OC4 Semisub model.

### 1.2.1-OFFSHORE WIND FARMS

Offshore wind farms represent one of the most promising solutions for large-scale renewable energy production. Located at sea, they take advantage of the stronger and more consistent winds found far from the coast, allowing them to generate more electricity than onshore wind farms. Additionally, by being situated often at significant distances from the shore, offshore wind farms contribute significantly to decarbonization without affecting the use of land for other purposes, such as agriculture or urban development.

Unlike onshore wind farms, offshore wind farms have certain advantages, such as reduced visual and acoustic interference with nearby communities. However, they also pose technical and logistical challenges. Installing turbines at sea involves a range of complications due to harsher conditions, such as wave dynamics, salt corrosion, and the need for specialized infrastructure for the transportation and installation of equipment.

There are different types of offshore installations, including floating turbines and fixed-bottom turbines. Floating turbines are becoming an increasingly viable option, especially in deep waters where fixed platforms cannot be constructed. These turbines are anchored to the seabed with mooring lines, enabling them to operate in deeper areas.

The growth of offshore wind farms has been significant in recent years, particularly in Europe, where countries like the United Kingdom, Denmark, Norway and Germany have invested heavily in this technology. In particular, the development of offshore wind farms in the North Sea has been a key driver of wind energy expansion in the region. However, the expansion of these types of farms is also being promoted in other parts of the world, such as the United States, China, and Japan, where different technological and policy solutions are being explored to harness the potential of offshore winds.

In addition to their ability to generate clean energy, offshore wind farms can serve as a driver of economic development in coastal regions, creating jobs both during the construction phase and in the operation and maintenance of the farms. This sector is fostering innovation in marine technologies and could be crucial for achieving global greenhouse gas emission reduction targets.

### 1.2.2-DIFFERENT TYPES OF OFFSHORE WIND TURBINES

Offshore wind turbines are primarily classified based on the orientation of their axis and the type of support used for installation in marine environments. These technologies have significantly evolved to adapt to the specific conditions of the oceanic environment and maximize energy efficiency.

### 1.2.2.1-BASED ON AXIS ORIENTATION

#### Horizontal Axis Wind Turbines (HAWT)

These are the most common type in offshore applications. Their rotational axis is parallel to the ground, and the blades rotate perpendicular to the wind. This design enables high energy capture efficiency due to its ability to harness strong and consistent winds. Additionally, HAWTs are easier to scale for large installed capacities (Jonkman et al., 2009).

However, they also face challenges, such as requiring a yaw system to align with the wind direction and mitigate the impact of dynamic loads on the blades.

#### Vertical Axis Wind Turbines (VAWT)

Although less common in marine environments, VAWTs offer unique advantages, such as the ability to capture wind from any direction without needing a yaw system. Their simplified design makes them more suitable for areas with more variable wind conditions. However, they exhibit lower aerodynamic efficiency and are generally better suited for specific applications or in combination with horizontal-axis systems (Islam, Mekhilef, & Saidur, 2013).

The following image (illustration 2) shows an example of a horizontal-axis wind turbine and a vertical-axis wind turbine.



*Illustration 2-HAWT and VAWT*

### 1.2.2.2-BASED ON SUPPORT TYPE

#### Fixed-Bottom Wind Turbines

These systems are used in waters with depths of less than 50 meters and are directly anchored to the seabed.

- Monopiles: Consist of a single steel column driven into the seabed. They are suitable for depths of up to 30 meters and are widely used due to their simplicity and low cost.

- Gravity-Based Structures: These use heavy concrete or steel bases that rest directly on the seabed. They require seabed preparation and are ideal for soils with good bearing capacity.

- Jackets: These are metallic lattice structures, similar to oil platforms, that provide greater stability in waters up to 50 meters deep. Their design helps reduce environmental impacts on the seabed (Musial & Butterfield, 2004).

The following image (illustration 3) shows, from left to right, the different types of fixed-bottom wind turbine foundations (Monopiles, Gravity-Based Structures, Jackets).



*Illustration 3-Fixed-Bottom wind turbines*

#### Floating Wind Turbines

Designed for deep waters (more than 50 meters), where fixed-bottom foundations are not feasible.

- Semi-Submersible Platforms: These structures remain afloat using a combination of buoyancy and ballast. Their design minimizes vertical and rotational movements, making them stable even in intense wave conditions.

-Spar Buoys: These consist of a cylindrical structure extending deep underwater to ensure stability through a low center of gravity.

-Tension Leg Platforms (TLP): Floating platforms anchored to the seabed with tensioned tendons. Their design reduces vertical movements and is ideal for intermediate depths (Jonkman & Matha, 2011).

The following image (illustration 4) shows, from left to right, the different types of floating wind turbines (TLP, Spar Buoys, Semi-Submersible Platform).

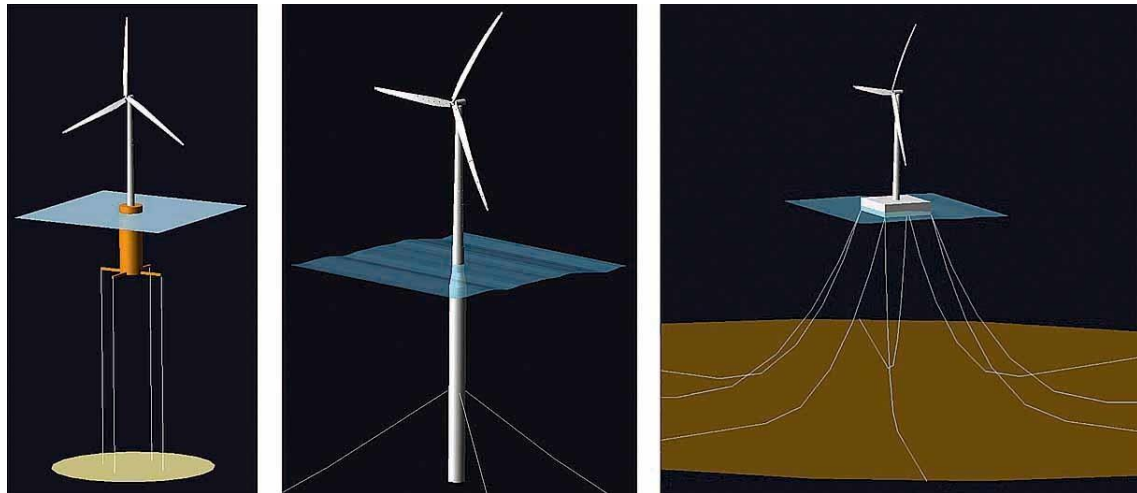


*Illustration 4-Floating wind turbines*

### 1.2.3-NREL 5MW OC4 SEMISUB

The model to be used (illustration 5) is a semi-submersible floating offshore wind system, which can be divided into two main components: the wind turbine (NREL 5MW) and the DeepCwind semi-submersible floating structure, as documented in the OC4 (Offshore Code Comparison Collaboration Continuation) project.

The NREL 5MW model is a widely used standard for offshore wind turbine simulations, making it ideal for research purposes due to the extensive availability of documentation.

The OC4 model includes specific data for structural, aerodynamic, and hydrodynamic evaluation, enabling detailed simulations of operational conditions.

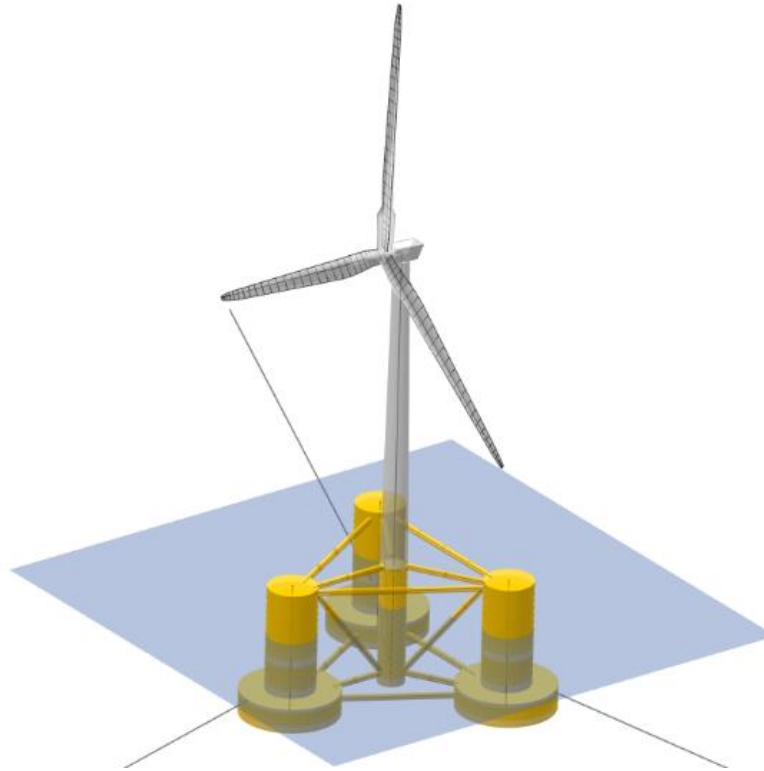


*Illustration 5-NREL 5MW OC4 SEMISUB model*

#### **1.2.2.1-TOWER PROPERTIES**

In summary, some of the characteristics of the tower in the model, extracted from the documents related to the project, are as follows:

- Location: The base of the tower is positioned 10 m above the still water level (SWL), while the top is 87.6 m above the SWL.

- Material: The tower is constructed from steel with an effective density of 8500 kg/m<sup>3</sup>, a Young's modulus of 210 GPa, and a shear modulus of 80.8 GPa.

- Geometry: The base diameter of the tower is 6.5 m, tapering to 3.87 m at the top. The wall thickness of the tower decreases linearly from 0.027 m at the base to 0.019 m at the top. The rotor has a diameter of 126 m.

#### **1.2.2.2- STRUCTURAL PROPERTIES OF THE FLOATING PLATFORM**

The floating platform consists of a central main column, which supports the tower and is connected to three secondary columns via pontoons and cross braces (illustration 6). The system also includes a mooring system anchored to the seabed, formed by three chains arranged symmetrically at 120° angles from one another, ensuring platform stability under environmental loads.

The main column has a diameter of 6.5 m (housing the tower), while the secondary columns have a diameter of 12 m at the top and 24 m at the bottom. These columns are spaced 50 meters apart, ensuring the platform stability. The main column and the secondary columns are connected by pontoons and braces with a diameter of 1.6 m. All these features can be seen below (illustration 7).



*Illustration 6-Floating platform*

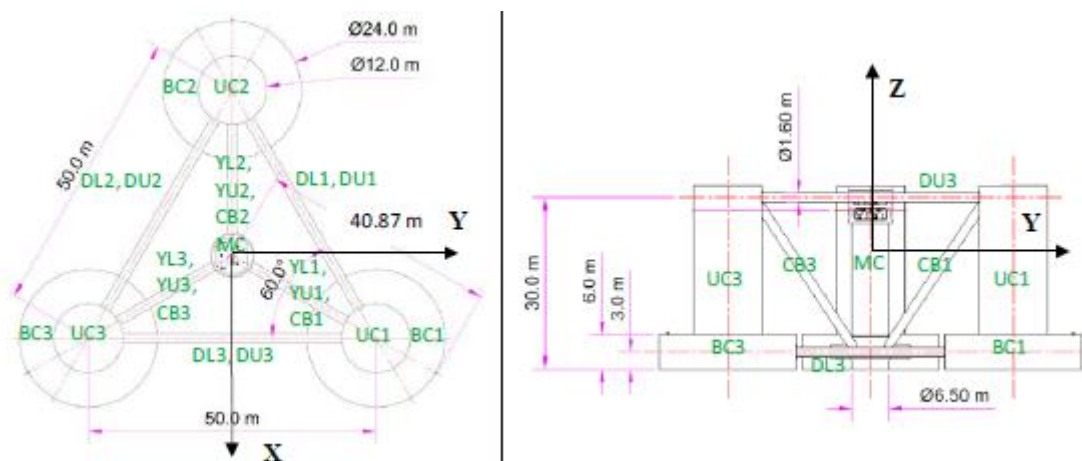


*Illustration 7-Features of the floating platform*

## 1.3 - PRINCIPLES OF WIND TURBINE OPERATION

This section outlines the physical and technological principles involved, as well as the theoretical and practical limitations affecting their performance.

### 1.3.1 - WIND ENERGY GENERATION

The basic principle behind a wind turbine is the extraction of energy from the wind through its blades, which rotate due to aerodynamic forces. This force depends directly on wind speed and blade geometry, designed to optimize the pressure difference



between the upper and lower surfaces. As explained by Iberdrola (2023), the resulting motion is transferred to the rotor, comprising a main shaft and an electric generator.

#### - Blade Aerodynamics:

The blades of a wind turbine are designed to maximize wind energy capture using aerodynamic principles. The wind generates two main forces:

Lift force: Caused by the pressure difference between the two surfaces of the blade.

Drag force: Resistance to the wind movement.

Optimal design seeks to maximize lift while minimizing drag. This balance is critical to achieving a high-power coefficient ( $C_p$ ), defined as the fraction of reference wind energy. For instance, the blades of the NREL 5MW model are made of lightweight, durable composite materials to withstand wind forces while minimizing the turbine overall weight (IRENA, 2021).

Conversion Process: The complete energy generation process involves the following stages:

-Wind capture: The blades rotate as they interact with the airflow.

-Mechanical conversion: The rotational motion of the hub is transferred to the low-speed shaft, which rotates at 7 to 20 revolutions per minute (RPM).

-Speed multiplication: A gearbox increases the rotational speed, enabling the generator to operate at a frequency of 1,500 RPM.

-Electrical conversion: The generator transforms mechanical energy into electrical energy. This component can be synchronous or asynchronous, depending on the turbine design.

### 1.3.2 - POWER CALCULATION AND EFFICIENCY

The reference wind energy used to evaluate the turbine power depends on three key factors: air density ( $\rho$ ), the swept area of the blades ( $A$ ), and the free stream wind speed ( $v$ ). According to the power equation:

$$P = \frac{1}{2} \rho A v^3 C_p$$

Where:

- $P$  is the generated power,



- $\rho$  is the air density,
  - $A$  is the rotor's swept area,
  - $v$  is the free stream wind speed, and
  - $C_p$  is the power coefficient.
- Air Density: Air density varies with altitude, temperature, and pressure. In marine environments, density is higher due to lower altitude and higher humidity, which enhances energy production.
  - Swept Area: The swept area is proportional to the square of the rotor radius. Larger-diameter turbines generate more energy but require more robust structures.
  - Wind Speed: Power generation depends on the cube of wind speed, meaning small variations in wind speed have a significant impact on energy output.
  - Efficiency and Theoretical Limits: According to Betz's limit, no wind turbine can produce more than 59.3% of the reference wind kinetic energy. Modern turbines achieve  $C_p$  values between 0.4 and 0.5, accounting for aerodynamic, mechanical, and electrical losses.

## 1.4-CLIMATIC CONDITIONS AT SEA

Since the marine environment presents special conditions, wind turbines must be designed to withstand factors such as wind, waves, salinity, and temperature.

### 1.4.1-OCEAN WINDS

Winds are stronger and more consistent offshore than on land due to the low surface roughness of the ocean. This results in a more uniform airflow, enhancing the efficiency of wind turbines. According to Burton et al. (2011), offshore winds can achieve capacity factors exceeding 40%, significantly higher than the average for onshore installations.

However, these winds also present challenges, such as sudden gusts and intense storms. These extreme conditions impose additional dynamic loads on turbine structures. Designing floating wind turbines, such as the NREL 5MW, requires consideration of these fluctuations to ensure both stability and structural integrity.

### 1.4.2-OCEAN WAVES

Ocean waves are one of the main sources of dynamic loads affecting floating wind turbines. This phenomenon is generated by the transfer of energy from the wind to the sea surface and can be classified into two main types:

-Wind waves: Related to local winds, generating irregular waves with shorter wavelengths.

-Swell waves: Originating from distant storms, characterized by longer and more regular waves.

The height, frequency, and direction of the waves directly influence the stability and design of the floating platform. As explained by Molins et al. (2014), semisubmersible platforms, such as the one used by the NREL 5MW, are designed to minimize vertical motions (heave) and rotational oscillations (pitch and roll).

Hydrodynamic analysis of waves is essential to predict cyclic loads that can induce fatigue in structural components and affect the turbine lifespan.

### 1.4.3-INTERACTION BETWEEN WIND AND WAVES

The simultaneous interaction of wind and waves introduces additional complexities in the design and operation of offshore wind turbines. Combined loads can generate amplified motions in floating platforms, affecting both their stability and energy performance.

According to Jonkman et al. (2009), the design of the NREL 5MW model includes distributed mooring systems that mitigate the motions induced by wind-wave interactions. These systems consist of mooring lines and counterweights that stabilize the structure under rough sea conditions.

Additionally, the use of advanced hydrodynamic and aerodynamic simulations allows for predicting the dynamic behavior of turbines under combined wind and wave conditions, optimizing their design and operation.

### 1.4.4-CHALLENGES OF THE MARINE ENVIRONMENT: CORROSION AND MAINTENANCE

The marine environment is highly corrosive due to salinity and constant exposure to water. This phenomenon affects both the metallic components and electrical systems of wind turbines. As Fischer et al. (2010) pointed out, the materials used in these installations must include anti-corrosive coatings and resistant alloys to ensure an adequate service life.

Another significant challenge is maintenance. Offshore turbines are less accessible than onshore ones, increasing operational costs and complicating repairs. To mitigate these issues, manufacturers are developing remote monitoring technologies that allow faults to be detected before critical failures occur.

## 2-SIMULATION CODE

### 2.1-QBLADE

For the simulation and obtaining of results, the program QBlade was used, an open-source software designed for the analysis, simulation and support in the design of wind turbine. It is primarily used in wind energy research and technology development and is highly useful due to its integration with aerodynamic and structural calculation tools. QBlade is built on the open-source library XFOIL, which enables efficient and accurate aerodynamic profile calculations.

One of QBlade's most notable features is its capability to perform BEM (Blade Element Momentum) simulations, a classical method widely used to predict the performance of wind turbines. Additionally, it supports dynamic simulations of turbine loads and behavior under variable wind and other environmental conditions, such as wave action.

Key QBlade tools that will be discussed in more detail include:

- Aerodynamic profile design.
- Analysis of aerodynamic profiles.
- 360° polar extrapolation.
- Blade design.
- BEM analysis.
- Definition of the turbine and its structure.
- Simulation.

### 2.2- INTRODUCTION TO THE PROGRAM

The main objective to be achieved in the program has been the design of the existing NREL 5MW OC4 Semisub wind turbine model. The primary purpose of this chapter is to provide a description of both the modeling and simulation process that must be carried out, as well as the different methods used within the program.

#### 2.2.1-AERODYNAMIC PROFILE DESING

The first step in modeling our wind turbine is to generate the different airfoils that will make up the blades. For this, we have two options: importing a pre-designed airfoil by

downloading files from an existing model or generating airfoils using the program feature to create circular or NACA-type profiles. Using the table (illustration 8), the main characteristics of each airfoil can be deduced.

	Foil Name	Thickness (%)	at (%)	Camber (%)	at (%)	Points	LE Flap (deg)
1	Cylinder1_coords	100.00	49.70	0.00	0.00	399	0.00

*Illustration 8-Table of airfoil generator*

-Foil Name: Refers to the name of each airfoil, which can be a cylinder or more complex profiles such as those from the DU series (commonly used in wind turbine aerodynamics).

-Thickness (%): Represents the maximum thickness of the airfoil, expressed as a percentage of the chord (the horizontal distance from the leading edge to the trailing edge). A thickness of 100% corresponds to a circular geometry. Following the maximum thickness value, "at(%)" indicates the relative position of the maximum thickness along the chord starting from its leading edge. In a circular profile, this value is 50%, while in aerodynamic profiles, the maximum thickness tends to be closer to the leading edge (values less than 50%).

-Camber (%): Indicates the degree of curvature of the airfoil, expressed as a percentage of the chord. A camber of 0% means the airfoil is symmetric, while positive values (e.g., 2%) indicate an upward curvature. After the camber value, "at(%)" specifies the position along the chord from the leading edge where the maximum curvature occurs, expressed as a percentage of the chord.

-Points: Represents the number of discrete points used to define the contour of the airfoil. A higher number of points allows for a more accurate representation but may increase computation time.

-LE Flap (deg): Refers to the deflection angle of the flap located at the leading edge of the airfoil, expressed in degrees.

In our case, since it is an already designed model, the only step required was importing the pre-uploaded airfoils, resulting in the output shown in the following image (illustration 9).

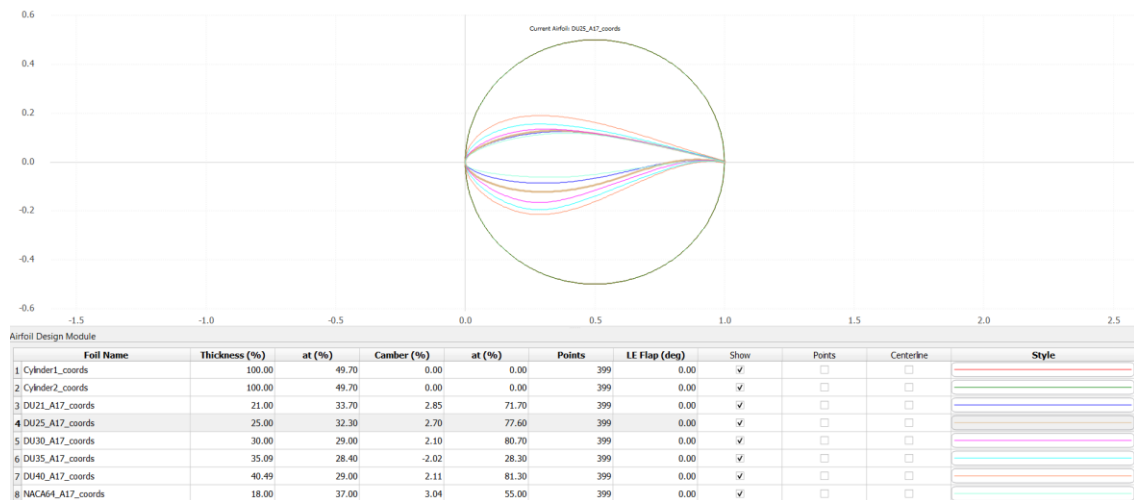


Illustration 9- Airfoils profiles from NREL 5MW

As can be observed, the blades of the NREL 5MW OC4 Semisub model feature 8 different airfoils. Among them, 2 are circular and correspond to the initial sections of the blade, while the remaining ones are from the DU series and belong to the aerodynamic portion of the blade.

## 2.2.2-ANALYSIS OF AERODYNAMIC PROFILES

Once all the aerodynamic profiles have been generated, we can proceed to analyze them. This is done by accessing the "Airfoil Analysis Module," where an analysis can be performed for each of the different aerodynamic profiles created. The purpose of this is to understand the various characteristics and behaviors of these profiles.

This analysis the wind effects in terms a detailed view of how the aerodynamic profiles of the turbine blades respond to different angles of attack, pressure distributions, and operating conditions. Such insights are crucial for optimizing blade design and improving the turbine efficiency and stability.

It is important to note that this analysis only provides information for angles of attack within the range of  $[-20^\circ$  to  $20^\circ]$ . Therefore, an extrapolation will be necessary later, which will be explained in subsequent sections.

The results obtained from this analysis are shown in the following image (illustration 10).

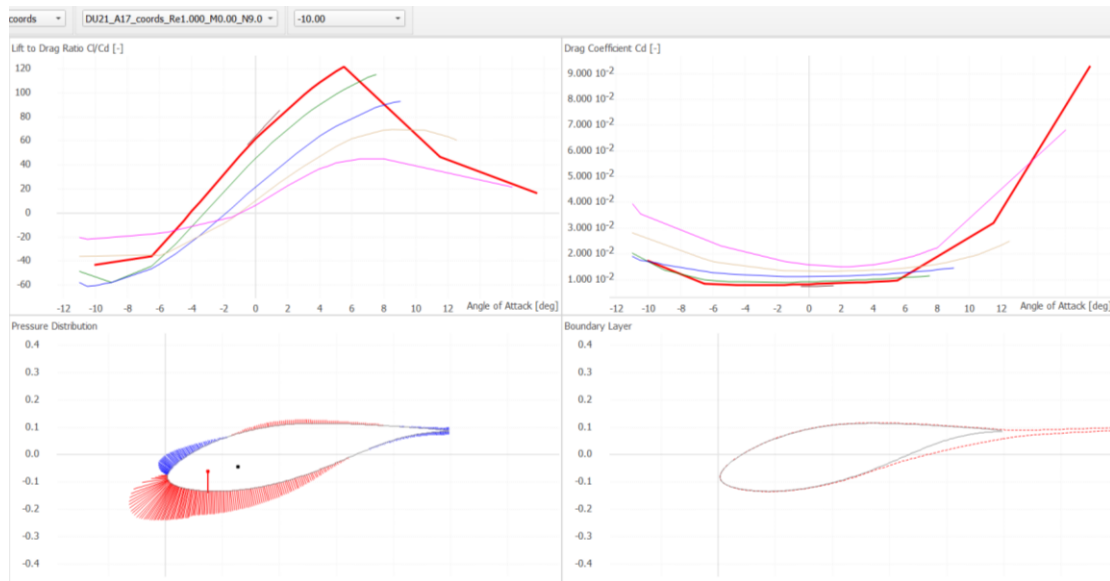


*Illustration 10-Analysis results*

Four graphs can be observed, with the top two representing curves for each profile. The most prominent curve corresponds to the profile “DU21\_A17\_coords”, while the bottom two graphs pertain exclusively to this profile. These graphs are the following:

1. Graph of the lift-to-drag ratio (also known as the blade efficiency) versus the angle of attack (illustration 11).
2. Graph of the drag coefficient versus the angle of attack (illustration 12).
3. Graph of pressure distribution along the aerodynamic profile (illustration 13).
4. Graph of the boundary layer (illustration 14).

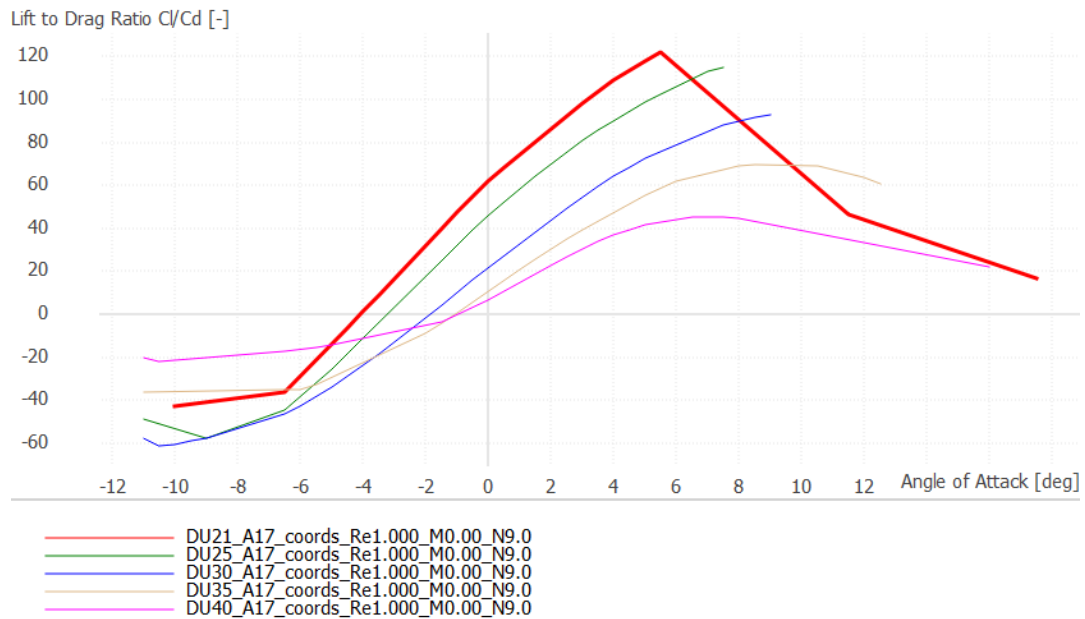
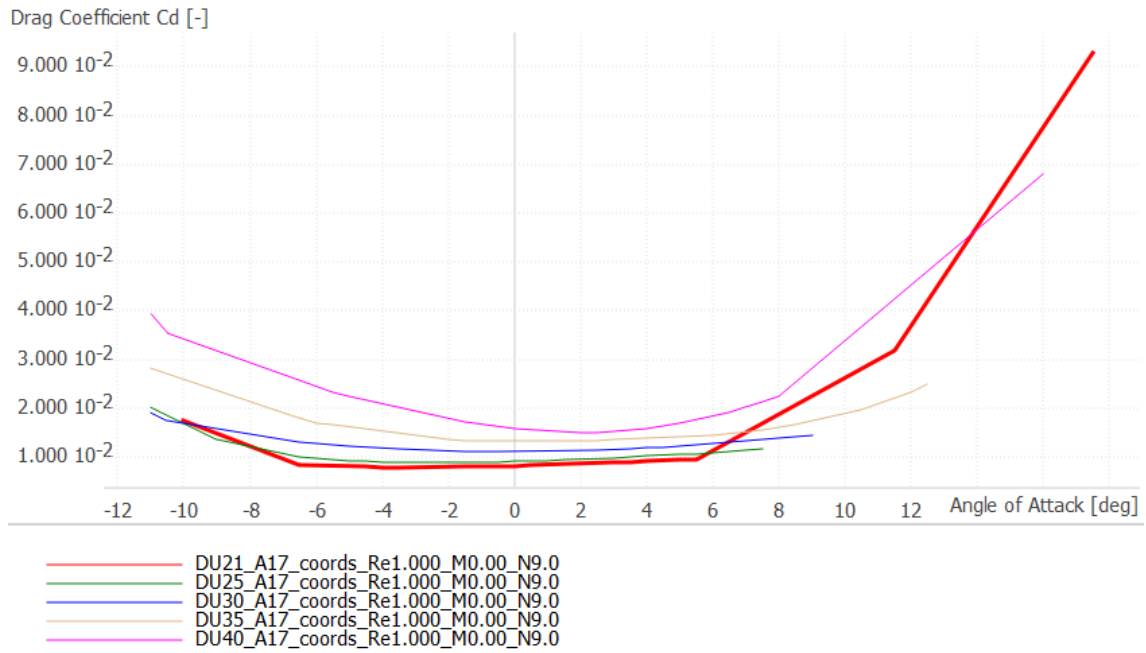


Illustration 11- Graph of the lift-to-drag ratio versus the angle of attack

-Y-Axis: Represents the ratio between the lift coefficient ( $Cl$ ) and the drag coefficient ( $Cd$ ) of the aerodynamic profile. This ratio is an indicator of aerodynamic efficiency; the higher the ratio, the more efficient the profile being analyzed.

-X-Axis: Represents the angle of attack, which is the angle between the direction of the relative flow velocity and the chord line of the aerodynamic profile.

As the angle of attack increases, the  $Cl/Cd$  ratio also increases up to a certain point, after which it begins to decrease. This peak represents the point of maximum aerodynamic efficiency, beyond which the profile enters a region of reduced efficiency due to flow separation. Each curve illustrates the  $Cl/Cd$  ratio for a different profile or operating condition, helping to identify the optimal angle of attack for each.



*Illustration 12- Graph of the drag coefficient versus the angle of attack*

-Y-Axis: Represents the drag coefficient ( $C_d$ ), which measures the aerodynamic drag generated by the profile. A low  $C_d$  value is desirable to minimize aerodynamic losses.

-X-Axis: As in the previous graph, it represents the angle of attack in degrees.

As observed, when the angle of attack increases from negative to positive values, the drag coefficient remains low until it reaches a point near  $0^\circ$  or  $5^\circ$ , after which it begins to rise rapidly. This behavior is expected, as at higher angles of attack, the airflow separates more easily from the profile, causing greater drag. Each colored curve represents a different profile, allowing for an analysis of how drag changes for each profile as a function of the angle of attack.



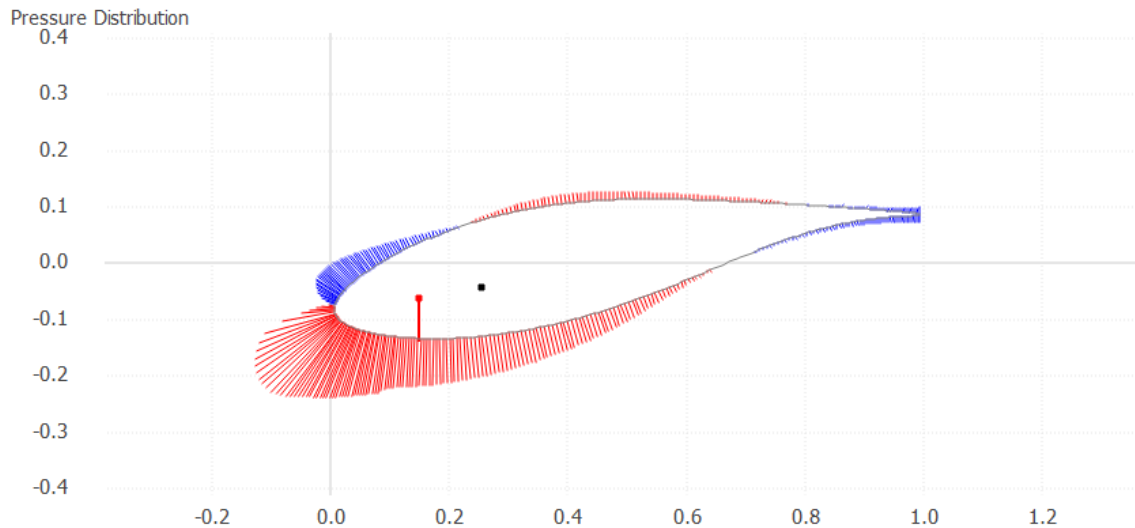


*Illustration 13- Graph of pressure distribution along the DU21\_A17 aerodynamic profile when  $\alpha = -10^\circ$*

-Y-Axis: Represents the pressure distribution along the aerodynamic profile. Positive values (in blue) and negative values (in red) indicate regions of high and low pressure, respectively, on the surface of the profile.

-X-Axis: Represents the position along the chord of the profile, from the leading edge (left) to the trailing edge (right).

This graph illustrates how pressure is distributed along the aerodynamic profile. The pressure vectors (arrows) indicate the magnitude and direction of the pressure acting on the profile. A greater pressure difference between the upper and lower surfaces generates lift. This analysis is essential for assessing the forces acting on the profile and optimizing its design to maximize lift and minimize drag.

In this specific case, the pressure distribution is shown for the DU21\_A17 profile at an angle of attack of -10 degrees. This graph can display all the studied profiles at various angles of attack used during the simulation.

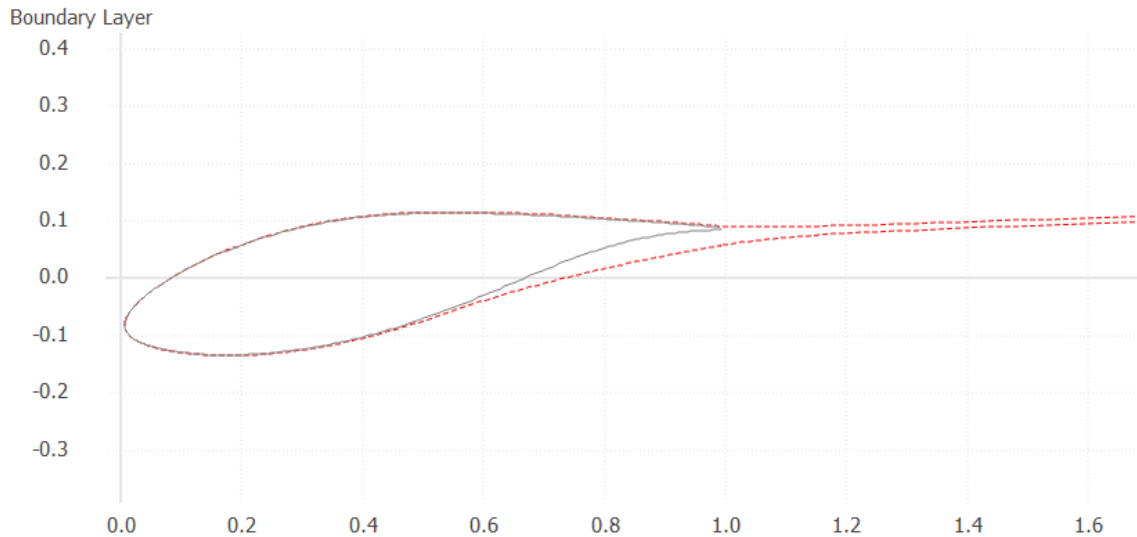


*Illustration 14- Graph of the boundary layer*

-Y-Axis: Represents the thickness of the boundary layer, the region near the surface of the profile where viscosity effects are significant, and the airflow slows down due to friction.

-X-Axis: Similar to the pressure distribution graph, it represents the position along the chord of the profile, from the leading edge to the trailing edge.

This graph illustrates how the boundary layer develops along the profile. As the airflow moves from the leading edge to the trailing edge, the boundary layer thickens due to friction. A thick boundary layer can indicate turbulent or near-separation airflow, which is critical for assessing the profile performance in terms of stability and aerodynamic efficiency.

### 2.2.3-POLAR EXTRAPOLATION TO 360°

As mentioned earlier, the initial analysis of the airfoils is only conducted for angles of attack between  $-20^\circ$  and  $20^\circ$ . Since the profiles in the simulation will be subjected to varying angles of attack determined by meteorological conditions, it is crucial to perform this extrapolation to understand the behavior of the airfoils beyond the previously measured angles.

The QBlade software allows for two different types of extrapolation methods to be employed: the Viterna method and the Montgomery method.

#### **Viterna Method**

Developed by L. A. Viterna and R. D. Corrigan in 1981, this method extrapolates the lift (Cl) and drag (Cd) coefficients of an airfoil to high angles of attack, including the stall and

post-stall regions. It relies on fitting available experimental data and applying empirical formulas to estimate aerodynamic behavior for unmeasured angles. This method is widely used due to its simplicity and effectiveness in predicting airfoil performance under extreme conditions.

## Montgomery Method

Proposed by J. S. Montgomery and K. C. Leung in 1989, this method also aims to extrapolate polar data to high angles of attack. Unlike the Viterna method, the Montgomery approach assumes that the aerodynamic profile behaves like a flat plate at high angles of attack. It uses specific fitting parameters to ensure the continuity and smoothness of the extrapolated lift and drag curves, offering an alternative to the Viterna method in certain applications.

For this simulation, the Viterna method was selected for extrapolation, yielding the following results (illustration 15).

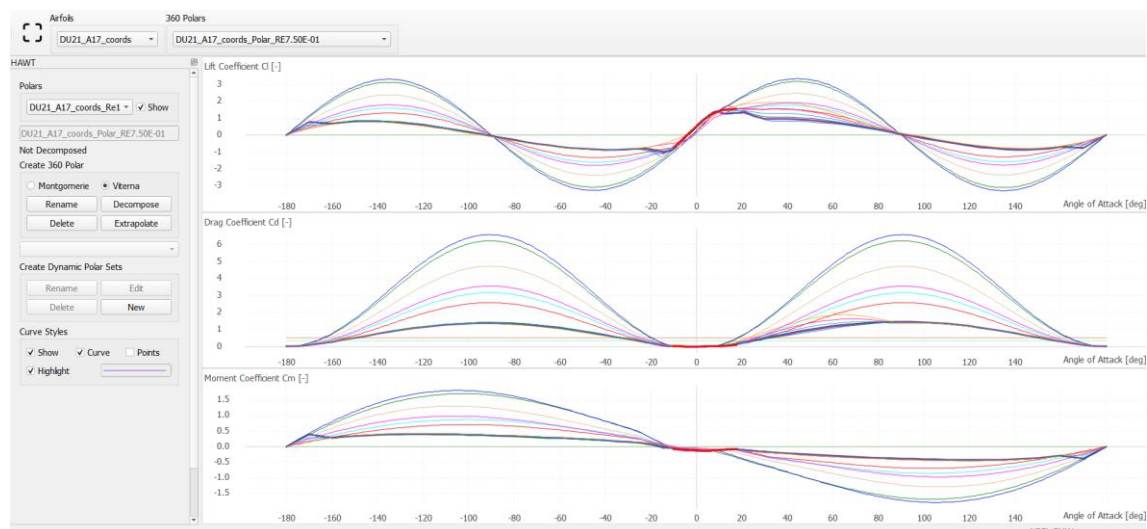


*Illustration 15- Results of the polar extrapolation*

We can observe three graphs:

### 1-Lift Coefficient vs. Angle of Attack

-Y-Axis: Represents the lift coefficient ( $C_l$ ), which indicates the amount of lift force generated by the airfoil as a function of the angle of attack.

-X-Axis: Represents the angle of attack in degrees, ranging from  $-180^\circ$  to  $180^\circ$ , which is a much broader range compared to conventional data (typically limited to between  $-20^\circ$  and  $20^\circ$ ).

Each curve corresponds to a studied airfoil, showing a symmetric and smooth shape, peaking at approximately  $\pm 90^\circ$ , which is characteristic of the Viterna extrapolation method. At extreme angles, especially near  $\pm 180^\circ$ , the lift decreases. The symmetry at extreme values indicates that the extrapolation method aims to maintain a physically reasonable behavior beyond the experimental data range.

## 2.Drag Coefficient vs. Angle of Attack

-Y-Axis: Represents the drag coefficient ( $C_d$ ), which measures the amount of drag force generated by the airfoil.

-X-Axis: Similar to the previous graph, it represents the angle of attack over the wide range of  $\pm 180^\circ$ .

Each curve corresponds to a specific airfoil profile, showing that the drag coefficient peaks around  $\pm 90^\circ$ . This is expected, as at these high angles of attack, the airflow fully separates from the airfoil, leading to significant drag. The shape of the curve suggests that the drag reaches its maximum when the flow is fully separated. This trend is both physical and expected, as at extreme angles, the profile presents a larger frontal area to the airflow.

## 3-Moment Coefficient vs. Angle of Attack

-Y-Axis: Represents the moment coefficient ( $C_m$ ), a dimensionless parameter that evaluates the torque on the airfoil due to the flow.

-X-Axis: Represents the angle of attack in degrees, within the same range of  $\pm 180^\circ$ . The moment coefficient shows a symmetric behavior around  $\pm 90^\circ$ . The  $C_m$  value transitions from positive to negative depending on the angle of attack. Its shape reflects how the distribution of forces on the airfoil changes as the angle of attack varies. This symmetry and the amplitude of the values are typical of extrapolations, indicating that the airfoil reaches a neutral point at certain angles. This is physically reasonable and provides valuable insights into the aerodynamic performance of the profiles under extreme conditions.

## 2.2.4-BLADE DESIGN

Once the complete analysis of the aerodynamic profiles has been carried out and both their geometry and characteristics are well-defined, the wind turbine blades can be

shaped. The QBlade application offers a user-friendly section specifically designed for blade modeling, providing intuitive tools for the process.

To generate wind turbine blades, there are two main options.

The first one is manual generation, which involves constructing the blades step by step by working with the table shown below (illustration 16). This table allows for the input of key parameters such as chord length, twist angle, and the distribution of profiles along the blade, enabling a precise and customized design tailored to the turbine specific requirements.

The second is to import real blade designs

	Pos [m]	Chord [m]	Twist [deg]	Foil	Polar
1	0.000	3.542	13.310	Cylinder1_coords	Cylinder1_coords_Polar...

*Illustration 16-Manual blade design option*

It works as follows: the first column corresponds to the position of the profile along the blade (0m indicates the first profile), the second column specifies the chord length of the profile, and the third column indicates the twist angle of the profile. Lastly, the fourth and fifth columns refer to the profile being used and the extrapolation method applied to it.

It can be seen below, on (illustration 17) all the characteristics of the blade.

	Pos [m]	Chord [m]	Twist [deg]	Foil	Polar
1	0.000	3.542	13.310	Cylinder1_coords	Cylinder1_coords_Polar...
2	1.367	3.542	13.310	Cylinder1_coords	Cylinder1_coords_Polar...
3	4.100	3.854	13.310	Cylinder1_coords	Cylinder1_coords_Polar...
4	6.833	4.167	13.310	Cylinder2_coords	Cylinder2_coords_Polar...
5	10.250	4.557	13.310	DU40_A17_coords	DU40_A17_coords_Pol...
6	14.350	4.652	11.480	DU35_A17_coords	DU35_A17_coords_Pol...
7	18.450	4.458	10.160	DU35_A17_coords	DU35_A17_coords_Pol...
8	22.550	4.249	9.010	DU30_A17_coords	DU30_A17_coords_Pol...
9	26.650	4.007	7.790	DU25_A17_coords	DU25_A17_coords_Pol...
10	30.750	3.748	6.540	DU25_A17_coords	DU25_A17_coords_Pol...
11	34.850	3.502	5.360	DU21_A17_coords	DU21_A17_coords_Pol...
12	38.950	3.256	4.190	DU21_A17_coords	DU21_A17_coords_Pol...
13	43.050	3.010	3.130	NACA64_A17_coords	NACA64_A17_coords_...
14	47.150	2.764	2.320	NACA64_A17_coords	NACA64_A17_coords_...
15	51.250	2.518	1.530	NACA64_A17_coords	NACA64_A17_coords_...
16	54.667	2.313	0.860	NACA64_A17_coords	NACA64_A17_coords_...
17	57.400	2.086	0.370	NACA64_A17_coords	NACA64_A17_coords_...
18	60.133	1.419	0.110	NACA64_A17_coords	NACA64_A17_coords_...
19	61.500	0.961	0.000	NACA64_A17_coords	NACA64_A17_coords_...

*Illustration 17-Blade characteristics*

This approach allows for the creation of countless blades with varying characteristics, and the program also provides optimization models to improve user-created profiles. For this simulation, as it involves an existing model, it was unnecessary to design new blades. Instead, the task was to import the existing blades, resulting in the following geometry (illustration 18).

### NREL\_5MW

Blade Length: 61.50 [m]

Rotor Diameter: 126.00 [m]

Swept Area: 12461.91 [m<sup>2</sup>]

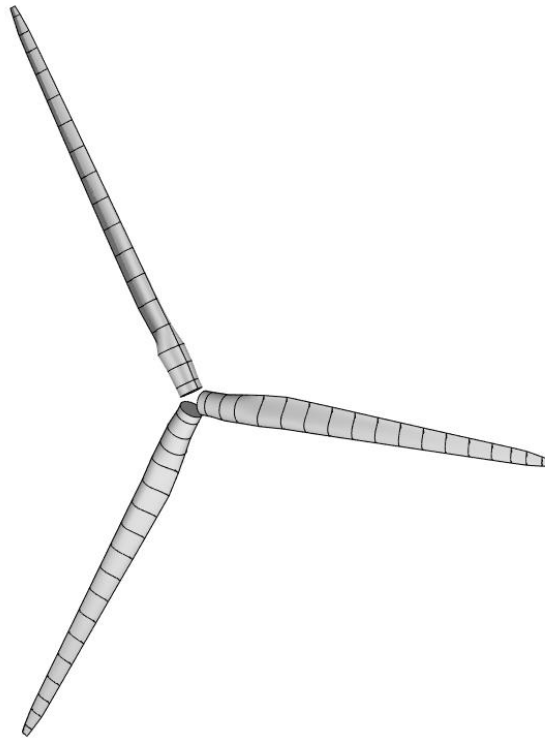
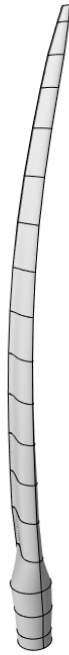


*Illustration 18 – NREL 5MW blades design*

Once the blade geometry has been created, this section of the program provides access to a feature that displays the first four modes of the blades along with their respective resonance frequencies (illustrations from 19 to 22).

NREL\_5MW: NREL\_5MW Structural Model

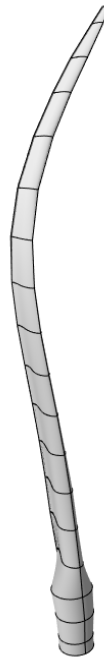


Blade Mass: 158476 kg

Flapwise Mode 1 Eigenfrequency: 0.67774 Hz

*Illustration 19- First mode*

NREL\_5MW: NREL\_5MW Structural Model

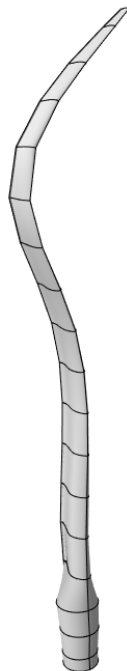


Blade Mass: 158476 kg

Flapwise Mode 2 Eigenfrequency: 2.05407 Hz

*Illustration 20-Second mode*

NREL\_5MW: NREL\_5MW Structural Model

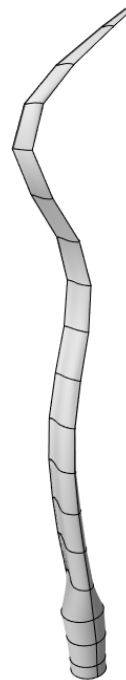


Blade Mass: 158476 kg

Flapwise Mode 3 Eigenfrequency: 4.4455 Hz

*Illustration 21-Third mode*

NREL\_5MW: NREL\_5MW Structural Model



Blade Mass: 158476 kg

Flapwise Mode 4 Eigenfrequency: 7.90856 Hz

*Illustration 22-Fourth mode*

This information is crucial during the construction of wind turbines, as they will be exposed to various frequencies caused by waves and wind. These resonance



frequencies must be considered when designing the platforms and the tower to ensure the structural integrity and operational stability of the turbine.

### 2.2.5- BEM ANALYSIS

The BEM (Blade Element Momentum) analysis module enables aerodynamic simulations with very low computational cost, short execution times, and generally accurate preliminary results regarding blade performance. This module is particularly useful for an initial evaluation of the blade model.

#### **Principles of BEM Analysis**

The BEM method divides each rotor blade into discrete radial sections, treating them as two-dimensional aerodynamic profiles. For each section, the lift and drag forces are calculated based on the angle of attack and the profile characteristics. These forces are balanced with the changes in axial and angular momentum of the airflow passing through the section, according to momentum theory. This equilibrium allows the determination of the load distribution along the blade and, consequently, the estimation of the turbine generated power.

#### **Applications of BEM Analysis**

1. **Blade Design:** BEM is essential in wind turbine blade design as it allows the optimization of blade geometry to maximize energy efficiency and minimize structural loads. By predicting how different profiles and configurations affect performance, engineers can develop blades that operate optimally under varying wind conditions.
2. **Performance Evaluation:** This method facilitates the estimation of a turbine power curve, which shows the relationship between wind speed and power output. This is crucial for assessing the economic and energy feasibility of wind energy projects.
3. **Load Analysis:** BEM helps determine the aerodynamic loads acting on the blades, which is critical for structural analysis and estimating the lifespan of turbine components.
4. **Simulation of Operational Conditions:** The method allows the simulation of turbine behavior under different wind conditions, including turbulence and directional changes. This is vital for ensuring operational stability and safety.

## Limitations and Considerations

Although BEM is a powerful tool, it has limitations, particularly in complex flow conditions such as wake interactions or high angles of attack. In such cases, it may be necessary to complement BEM with more advanced methods, such as Computational Fluid Dynamics (CFD) simulations or free vortex theories, to achieve more accurate results.

In the Rotor BEM submodule, users can perform rotor blade simulations across a range of Tip Speed Ratios (TSR). When defining a rotor simulation in the Analysis Settings panel, users can select the desired corrections (Corrections) for the BEM algorithm and simulation parameters. Once a simulation is defined, the user can specify a TSR range and the incremental step for the simulation.

Rotor simulations are always conducted with non-dimensional arguments. It is assumed that the free-stream velocity is uniform, and the rotor radius is normalized for the calculations. This means that dimensional power curves or load must be computed in post-processing.

After analyzing the blades performance using this module for a wind speed of 10 m/s, the following results were obtained (illustration 23).

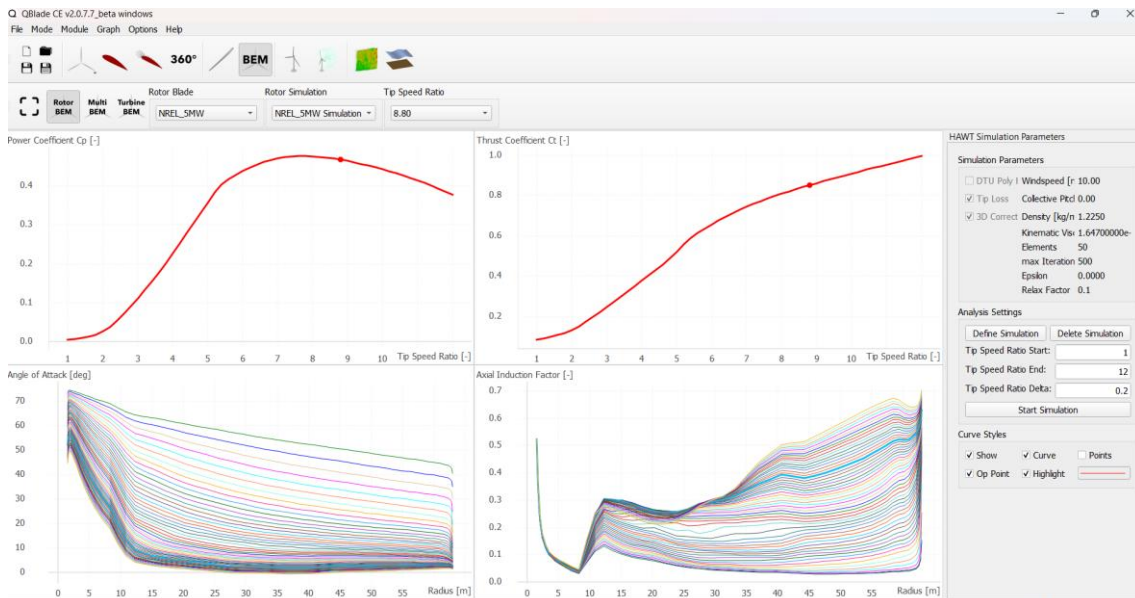


*Illustration 23-BEM Analysis for NREL 5MW at 10m/s*

In this image, four graphs are presented:

1. Graph of Power Coefficient ( $C_p$ ) versus Tip Speed Ratio (TSR) (illustration 24).

2. Graph of Thrust Coefficient ( $C_t$ ) versus Tip Speed Ratio (TSR) (illustration 25).
3. Graph of Angle of Attack versus Radius (illustration 26).
4. Graph of Axial Induction Factor versus Radius (illustration 27).

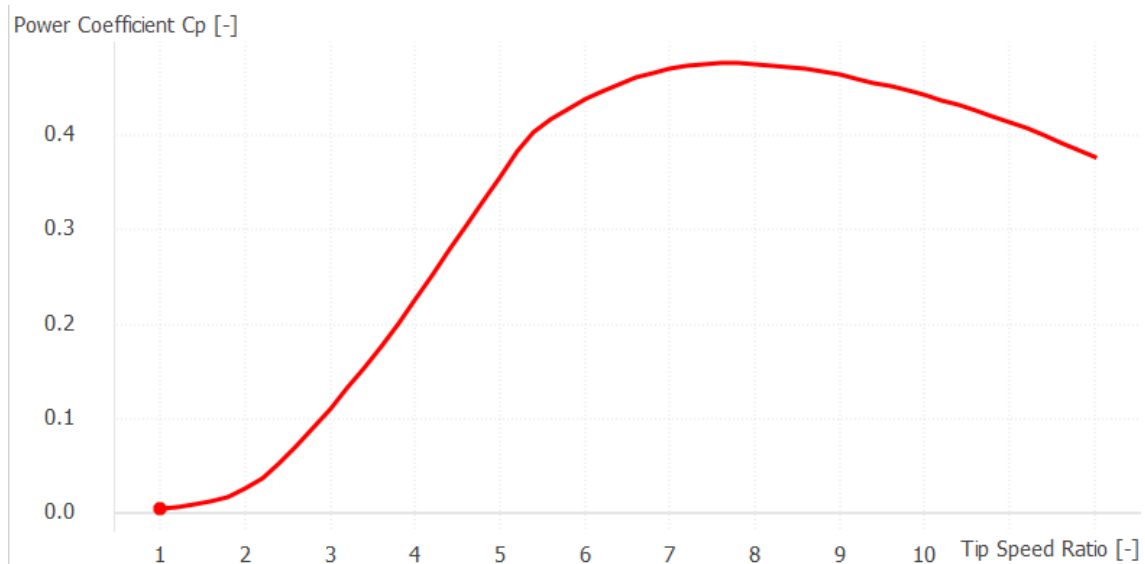


*Illustration 24- Graph of Power Coefficient ( $C_p$ ) versus Tip Speed Ratio*

-Y-Axis: Represents the power coefficient  $C_p$ , which is the ratio of the useful power generated by the rotor to the wind power available in the swept area of the blades. This coefficient is critical for determining the performance of the wind turbine.

-X-Axis: Represents the Tip Speed Ratio (TSR), which is the ratio of the tangential speed at the blade tip to the incoming wind speed.

As TSR increases,  $C_p$  also rises, reaching a maximum before decreasing. This peak represents the point of highest performance for the wind turbine. A high  $C_p$  value close to 0.5 or 0.45 is considered good since the theoretical limit (Betz Limit) is about 0.59.

The Betz Limit, also known as the Lancaster-Betz-Zhukovsky Limit, is the theoretical maximum performance a wind turbine can achieve when extracting energy from the wind. It establishes that, under ideal conditions, a turbine cannot capture more than 59.3% of the kinetic energy in a wind crossing a surface equal to the turbine swept area. This limitation arises because extracting energy slows the wind, but its velocity cannot drop to zero; otherwise, airflow through the turbine would cease.

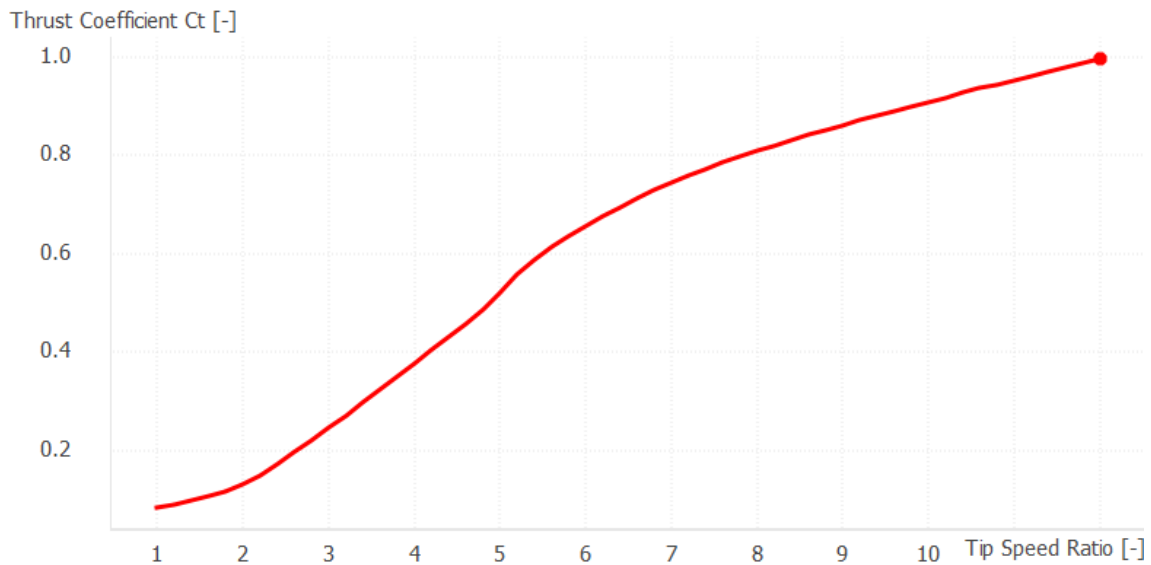


*Illustration 25- Graph of Thrust Coefficient ( $C_t$ ) versus Tip Speed Ratio*

-Y-Axis: Represents the thrust coefficient  $C_t$ , which measures the thrust force on the rotor relative to the wind force. This is important because a high  $C_t$  value can impact the turbine structure due to increased loading.

-X-Axis: As in the previous graph, the TSR represents the ratio of the blade tip speed to the wind speed.

In this graph,  $C_t$  increases with TSR and tends to stabilize around high values (close to 1). This suggests that as the rotor spins faster, the thrust force acting on it also increases, potentially raising the stresses on the system.

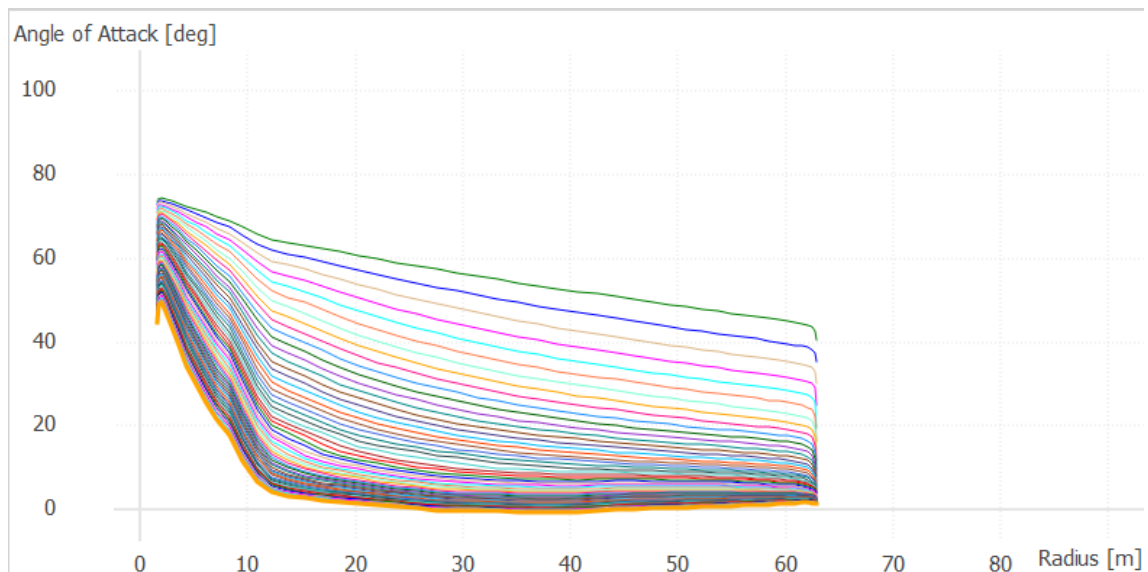


*Illustration 26- Graph of Angle of Attack versus Radius*

-Y-Axis: Represents the angle of attack in degrees, which is the angle between the relative wind velocity direction and the chord line of the blade airfoil. This angle is crucial because it influences the lift and drag generation.

-X-Axis: Represents the radial distance from the rotor center to the blade tip, measured in meters.

Each colored line corresponds to a different TSR value. It can be observed that near the blade root (close to the hub), the angle of attack is higher and tends to decrease toward the blade tip. This behavior is normal, as the relative velocity is lower near the root, requiring a higher angle of attack to generate the same lift force. This variation in the angle of attack along the radius ensures the blade profile remains efficient across its entire length.

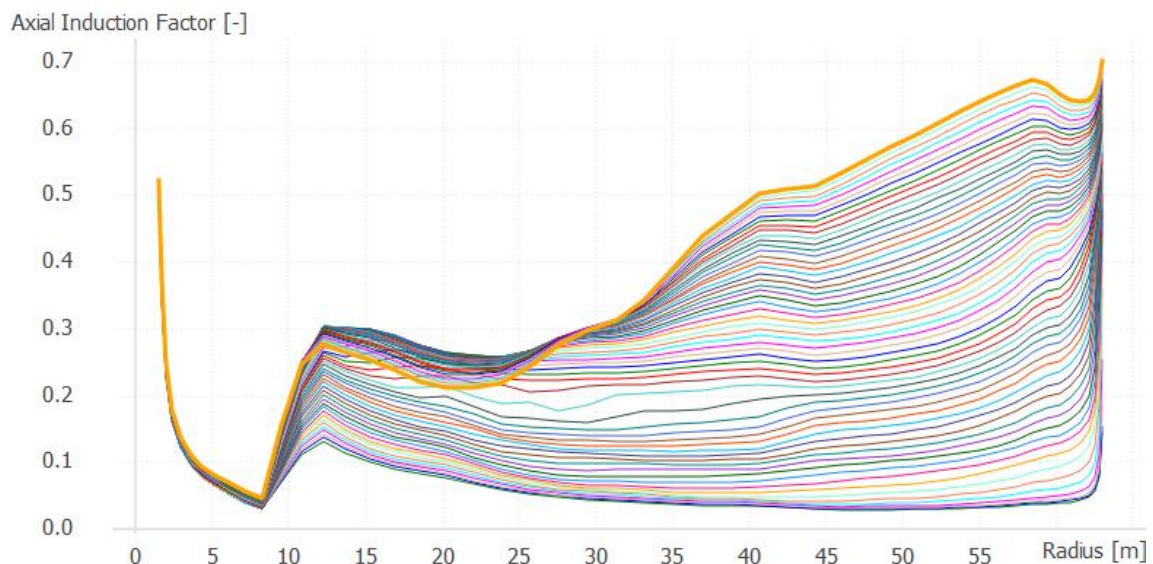


*Illustration 27- Graph of Axial Induction Factor versus Radius*

-Y-Axis: Represents the axial induction factor, which quantifies the reduction in wind speed caused by the presence of the rotor. A value of 0.33 indicates that the wind has slowed to two-thirds of its original speed, which is typical in wind turbine design.

-X-Axis: Similar to the previous graph, it represents the radial distance from the rotor center.

The axial induction factor varies along the radius for different TSR values (represented by different colors). Near the rotor center, the induction factor is higher due to greater wind interference. For low TSR values, the factor decreases toward the blade tip, which is normal since relative velocities and airfoil design affect the wind deceleration. For high TSR values, the axial induction factor exceeds 0.593 (Betz limit), potentially indicating aerodynamic overload, which could be detrimental to the blades.

After completing the BEM analysis, one can return to the blade design section and, using the QFEM submodule, analyze the loads experienced by the blade for various TSR values, such as TSR=1 (illustration 28) or TSR=12 (illustration 29).

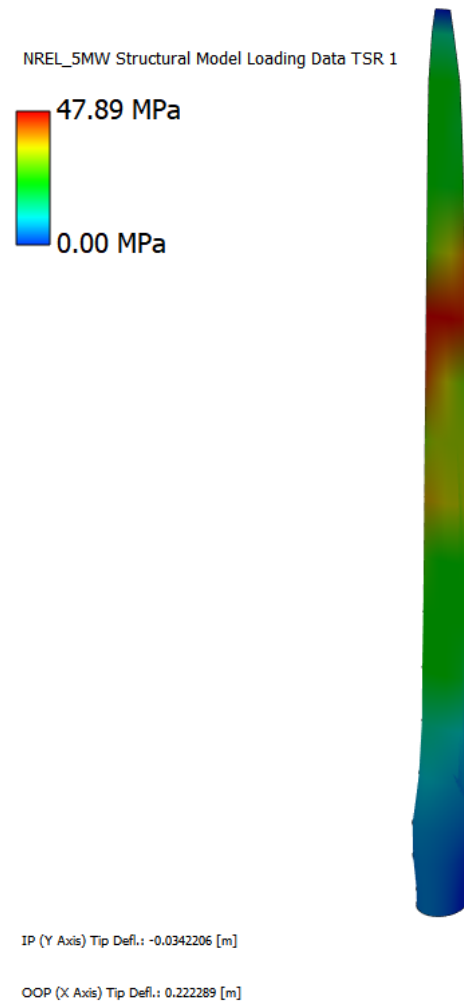


*Illustration 28-Load case when TSR=1*

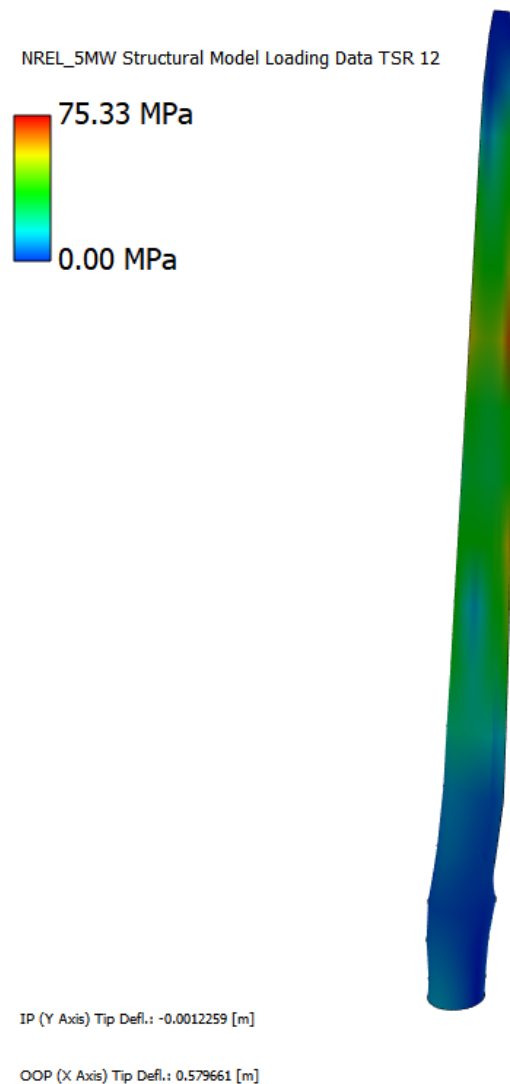


*Illustration 29-Load case when TSR=12*

As can be observed, for a TSR of 12, greater stresses are obtained compared to a TSR of 1, thus confirming the earlier comments regarding the influence of high TSR values on the blades when the wind speed is constant. This demonstrates that as the TSR increases, the aerodynamic and structural loads on the blades increase significantly, which can lead to higher stresses and potential risks to the wind turbine integrity.

We have to take into account that normally, the TSR is kept constant up to the nominal wind speed.

#### 4.2.6- DEFINITION OF THE TURBINE AND ITS STRUCTURE

Once the blades of our wind turbine have been defined and their corresponding BEM analysis has been conducted, the next step in the modeling process can be taken. In this section, both the turbine and the structure of the wind turbine can be defined. When a new turbine is generated, the following window appears (illustration 30).

The screenshot shows the 'Create a Turbine Definition' window in QBlade. The window is organized into several panels:

- Turbine Name and Rotor:** Includes fields for 'Turbine Name' (NREL\_5MW Turb), 'Blade Design' (NREL\_5MW), 'Turbine Type' (HAWT selected), 'Number of Blades' (3), 'Up- or Downwind' (Upwind selected), 'Rotor Rotation' (Standard selected), and 'Turbine Version Info' (View/Edit button).
- Wake Type:** Includes 'Wake Type' (Unsteady BEM selected), 'Unsteady BEM Parameters' (Azimuthal Polar Grid Discretization: 12, Include Tip Loss: On selected, Convergence Acceleration Time [s]: 0), and 'Dynamic Wake Meandering Model' (Enable Dynamic Wake Meandering: On selected).
- Turbine Geometry:** Includes fields for 'Rotor Overhang [m]' (10.5), 'Tower Height [m]' (90), 'Tower Top Radius [m]' (1.8), 'Tower Bottom Radius [m]' (2.52), 'Rotor Shaft Tilt Angle [deg]' (0), and 'Rotor Cone Angle [deg]' (0).
- Aerodynamic Discretization:** Includes 'Blade Panels' (30), 'Blade Disc Type' (COSINE), and 'Panel Interpolation' (LINEAR).
- Dynamic Stall:** Includes 'Dynamic Stall Model' (OYE) and 'Time constant Tf [-]' (8).
- Aerodynamic Models:** Includes checkboxes for 'Unsteady Attached Flow Aero' (On selected), 'Two Point L/D Correction' (On selected), 'Himmelskamp Effect' (On selected), 'Tower Shadow' (On selected), and 'Tower Drag Coeff. [-]' (0.5).
- Turbine Structural Model:** Includes 'Define Structural Model' (On selected), 'Main Structural Input File' (I\_DeepCWindSemi\_Main\_LPM), and buttons for 'View/Edit Struct.', 'View PotFlow', and 'Export Struct.'. It also has radio buttons for 'Aero. Loads' (Aero. Panels selected) and 'Struct. Nodes'.
- Turbine Controller:** Includes 'Controller Type' (TUB), 'Controller DLL' (TUBCon\_1.3.9\_64bit), and 'Controller Params.' (con\_Params\_V1.3.9\_NREL5MW). It has buttons for 'View/Edit Params.' and 'Export Params.'.
- Custom External Library:** Includes 'Function Call' (update), 'Exchange Array Size' (100), 'External Library List' (empty), and buttons for 'Add External Library' and 'Remove External Library'.

*Illustration 30-Window for turbine and structure modeling*

This QBlade window is designed to configure the specific parameters of a wind turbine and its operating environment before running a simulation. Each section allows for adjustments to critical elements of the turbine design and behavior, ensuring the model is as representative as possible of real-world conditions.

Since this is an existing model, the wind turbine structure is already defined in pre-downloaded files, so the only task is to load them into the (Turbine Structural Model) section. The same applies to the turbine itself, which is loaded into the (Turbine Controller) section.

Once both files have been loaded, the wind turbine can be created (illustration 31).



## NREL\_5MW Turb

### Aerodynamic Model

Wake Type: Polar BEM  
Total Aerodynamic Panels: 90  
Hub Height: 90.00 [m]

### Structural Model

Structural Nodes: 356  
Total Degrees of Freedom: 2399

### System Mass

Blade 1 Mass: 1.7734e+04 [kg]  
Blade 2 Mass: 1.7734e+04 [kg]  
Blade 3 Mass: 1.7734e+04 [kg]  
Nacelle & Hub Mass: 2.9678e+05 [kg]  
Total RNA Mass: 3.4998e+05 [kg]

Tower Mass: 2.4973e+05 [kg]

Substructure Member Mass: 5.1383e+02 [kg]  
Substructure M\_HYDRO Mass: 1.3473e+07 [kg]  
Total Substructure Mass: 1.3474e+07 [kg]

Mooring Cable Mass: 2.7805e+05 [kg]  
Total WT System Mass: 1.4346e+07 [kg]

### COG Positions

RNA COG: (-0.406, -0.000, 89.566) [m]  
RNA COG in Tower Top Coordsys: (-0.406, -0.000, 1.966) [m]  
Tower COG: (-0.000, -0.000, 43.379) [m]  
RNA + Tower COG: (-0.237, -0.000, 70.333) [m]  
Total Substructure COG: (-0.000, 0.000, -13.460) [m]  
Total WT System COG: (-0.010, -0.000, -9.889) [m]

### Controller

Type: TUB  
Controller File: TUBCon\_1.3.9\_64Bit  
Parameter File: TUBCon\_Params\_V1.3.9\_NREL5MW.xml

### Floating Installation

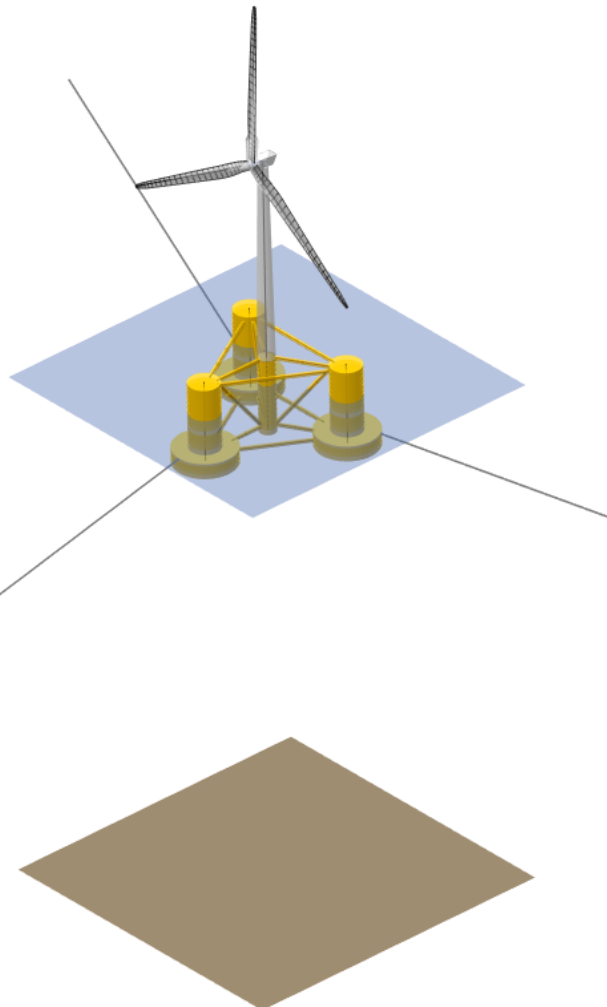


*Illustration 31-NREL 5MW OC4 Semisub model*

In this illustration, we can see the image of the wind turbine displayed by QBlade, along with its most important structural properties.

## 4.2.7-SIMULATION

The next and final step consists of running the simulation to obtain the results of the wind turbine performance. When starting a new simulation, the following window appears (illustration 32).

The image shows the QBlade simulation configuration window, which is divided into several tabs. The 'General Simulation Settings' tab is active, showing parameters for a 'New Turbine Simulation'. Key settings include a time step size of 0.027489141789, 1000 time steps, and a simulation length of 27.489 seconds. The 'Turbine Setup' tab shows the 'NREL\_5MW Turb' model with a rotational speed of 12.126 RPM and a TSR of 7.9999. The 'Turbine Environment' tab shows an offshore installation with a water depth of 200m. The 'Wind Boundary Condition' tab shows a uniform wind input type with a wind speed of 10 m/s. The 'Environmental Variables' tab shows physical constants like gravity (9.80665 m/s^2) and air density (1.225 kg/m^3).

*Illustration 32-Simulation window*

This configuration window in QBlade allows the user to set the fundamental parameters for a detailed simulation of the wind turbine behavior, in this case, the NREL 5MW model in an offshore environment. The settings cover everything from general simulation aspects to specific environmental, wind, and structural behavior conditions of the turbine.

First, the general parameters are defined, such as the simulation name, total duration, time step size, and the number of time steps, which determine the temporal resolution of the results. Additionally, the structural initialization of the turbine is configured, including ramp time to avoid abrupt transients and damping factors to improve model stability.

The wind conditions section is crucial for simulating the aerodynamic environment. Here, the wind speed, profile type (uniform or turbulent), and the wind model used, such as the power law, are specified, along with parameters like terrain roughness and reference height. This data are critical for obtaining accurate results regarding the aerodynamic loads on the rotor.

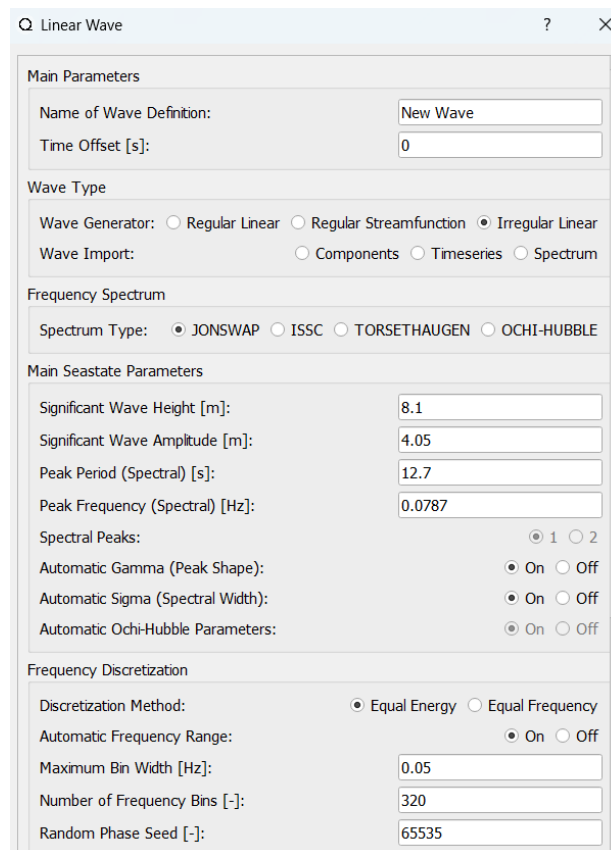
The turbine configuration includes defining the wind turbine model, in this case, the NREL 5MW, as well as rotor rotation parameters, the TSR (Tip Speed Ratio), and initial conditions, such as azimuth, pitch, and possible translations of the hub or floater. This enables adapting the simulation to the expected behavior of the turbine in different scenarios.

The turbine environment is described through parameters such as water depth, wave model, and ocean current conditions. These settings are essential for accurately simulating the dynamic effects in an offshore environment.

Finally, environmental variables such as gravity, air and water densities, and viscosities allow the physical model to be adjusted to precisely reflect real conditions. The window also permits the inclusion of external forces, such as hydrodynamic or aerodynamic ones, and loading custom files to simulate specific events or external conditions.

## 2.2.8-WAVE GENERATOR

For the wave model that will be used in the simulation, there is another section within QBlade that allows one to create different wave scenarios for the simulations. When generating a new scenario, the following window appears (illustration 33).



The screenshot shows the 'Linear Wave' window in QBlade. It contains several sections for configuring wave parameters:

- Main Parameters:**
  - Name of Wave Definition: New Wave
  - Time Offset [s]: 0
- Wave Type:**
  - Wave Generator: ☐ Regular Linear ☐ Regular Streamfunction ☒ Irregular Linear
  - Wave Import: ☐ Components ☐ Timeseries ☐ Spectrum
- Frequency Spectrum:**
  - Spectrum Type: ☒ JONSWAP ☐ ISSC ☐ TORSETHAUGEN ☐ OCHI-HUBBLE
- Main Seastate Parameters:**
  - Significant Wave Height [m]: 8.1
  - Significant Wave Amplitude [m]: 4.05
  - Peak Period (Spectral) [s]: 12.7
  - Peak Frequency (Spectral) [Hz]: 0.0787
  - Spectral Peaks: ☒ 1 ☐ 2
  - Automatic Gamma (Peak Shape): ☒ On ☐ Off
  - Automatic Sigma (Spectral Width): ☒ On ☐ Off
  - Automatic Ochi-Hubble Parameters: ☒ On ☐ Off
- Frequency Discretization:**
  - Discretization Method: ☒ Equal Energy ☐ Equal Frequency
  - Automatic Frequency Range: ☒ On ☐ Off
  - Maximum Bin Width [Hz]: 0.05
  - Number of Frequency Bins [-]: 320
  - Random Phase Seed [-]: 65535

*Illustration 33-Wave generator window*

Thanks to this window, waves can be generated with the characteristics desired, selecting the type of wave, the frequency spectrum, the spectrum period, and its height, among others. Once the wave is generated, something like what is shown in the following image (illustration 34) is obtained.

## H0.5T5\_ISSC

Significant Wave Height: 0.50 m  
Peak Period: 5.00 s  
Number of wave components: 347

### Wave Type

ISSC (Pierson-Moskowitz)  
Frequency Bins: 320

### Directional Spectrum

Unidirectional  
Principal Wave Direction: 0.00 deg

0.50 m/s  
Elevation  
-0.50 m/s

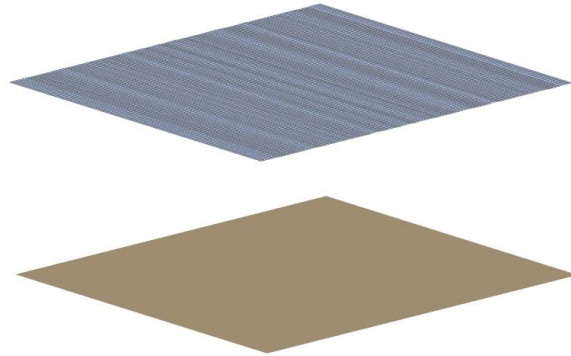


*Illustration 34-Wave spectrum generated*

### 3-SIMULATIONS

The main idea adopted in the work is to generate a combination of scenarios that reflect the possible conditions a floating wind turbine could face, off the coast of Bari. These simulations aim to cover a wide range of situations, from operating scenarios in favorable weather conditions to extreme situations that test the system design limits.

To achieve this, data was gathered from various websites that provide information on both wind and wave conditions in the region. For better understanding, these data have been organized into two tables, one for the wind and the other for the wave conditions:

1. **Wind conditions table (illustration 35):** Includes wind speed, horizontal direction, and vertical tilt.
2. **Wave conditions table (illustration 36):** Defines parameters such as significant wave height, peak period, and the selected spectrum to characterize the wave conditions. Different spectra were included to reflect conditions of locally generated seas (JONSWAP, ISSC) and more complex situations (Torsethaugen, Ochi-Hubble).

Simulation	Wind velocity (m/s)	Horizontal direction (°)	Vertical direction (°)
1	5	45	0
2	6	60	2
3	7	90	5
4	8	120	3
5	9	180	0
6	10	200	4
7	4	240	1
8	5	270	2
9	7	300	0
10	12	330	3
11	3	30	0
12	9	120	5
13	11	270	2

*Illustration 35-Wind conditions table*

Simulation	Wave height (m)	Peak period (s)	Peak frequency (Hz)	spectrum
1	0.8	7	0.14	JONSWAP
2	1	8	0.125	JONSWAP
3	1.2	10	0.1	JONSWAP
4	1.5	11	0.09	ISSC
5	1.8	12	0.083	JONSWAP
6	2	12	0.083	JONSWAP
7	0.6	6	0.166	ISSC
8	1	8	0.125	TORSETHAUGEN
9	1.3	9	0.111	OCHI-HUBBLE
10	2.5	14	0.071	JONSWAP
11	0.5	5	0.2	ISSC
12	1.8	10	0.1	TORSETHAUGEN
13	2.2	12	0.083	JONSWAP

*Illustration 36-Wave conditions table*

## 3.1-EXPLANATION OF DATA CHOICE AND RESULTS

### 3.1.1-EXPLANATION OF DATA CHOICE

#### 3.1.1.1-Simulation 1

-Wind Speed: 5 m/s, represents a light breeze, typical in good weather conditions on the Adriatic coast.

-Horizontal Direction: 45° (Northeast), common in Bari, where northeastern winds like the Bora can be frequent but not intense.

-Significant Wave Height: 0.8 m, corresponds to moderate local wave conditions.

-JONSWAP Spectrum: Ideal for local storms and semi-enclosed seas like the Adriatic.

#### 3.1.1.2-Simulation 2

-Wind Speed: 6 m/s, a slightly windier condition, still representative of moderate wind days.

-Horizontal Direction: 60°, simulates a variation in the predominant northeastern direction, indicating a possible wind rotation.

-Significant Wave Height: 1.0 m, more developed waves, generated by the increased wind speed.

-JONSWAP Spectrum: Useful for simulating the development of storms in semi-enclosed areas.

#### *3.1.1.3-Simulation 3*

-Wind Speed: 7 m/s, represents a fresh breeze, common in more dynamic maritime conditions.

-Horizontal Direction: 45°

-Significant Wave Height: 1.2 m, compatible with the wind speed and a somewhat more pronounced wave.

-JONSWAP Spectrum: Maintains suitability for closed seas with moderate energy.

#### *3.1.1.4-Simulation 4*

-Wind Speed: 8 m/s, a strong and consistent wind, representative of local storms in Bari.

-Horizontal Direction: 120°, simulates an oblique angle from the southeast, typical of the Scirocco wind.

-Significant Wave Height: 1.5 m, higher waves, consistent with strong and persistent winds.

-ISSC Spectrum: Suitable for developing waves with a single spectral peak.

#### *3.1.1.5-Simulation 5*

-Wind Speed: 9 m/s, a very strong wind, frequent during more intense storms in the Adriatic.

-Horizontal Direction: 180° (South), represents a wind from the south, possibly with warm Mediterranean air.

-Significant Wave Height: 1.8 m, a significant wave generated by a moderate storm.

-JONSWAP Spectrum: Ideal for simulating semi-enclosed seas with high energy.

#### *3.1.1.6-Simulation 6*

-Wind Speed: 10 m/s, an extreme wind condition that can occur during intense storms or in the open sea.

-Horizontal Direction: 200°, reflects strong winds from the southwest, common in transitioning storm conditions.

-Significant Wave Height: 2.0 m, very developed waves, suitable for evaluating the turbine's capacity in severe conditions.

-JONSWAP Spectrum: Allows simulation of agitated seas in semi-enclosed areas.

#### *3.1.1.7-Simulation 7*

-Wind Speed: 4 m/s, a light wind, typical of calmer waters on stable days.

-Horizontal Direction: 240°

-Significant Wave Height: 0.6 m, compatible with low winds and locally generated waves.

-ISSC Spectrum: Simplified and suitable for calm conditions.

#### *3.1.1.8-Simulation 8*

-Wind Speed: 5 m/s, light wind, but with possible rotation.

-Horizontal Direction: 270° (West), an occasional wind from the west, which may influence coastal currents.

-Significant Wave Height: 1.0 m, a moderate wave generated by consistent wind.

-TORSETHAUGEN Spectrum: Well-suited for transitions between local and remote waves.

#### *3.1.1.9-Simulation 9*

-Wind Speed: 7 m/s, a more dynamic condition with significant winds.

-Horizontal Direction: 300°, represents wind from the northwest.

-Significant Wave Height: 1.3 m, compatible with consistent winds and moderate seas.

-OCHI-HUBBLE Spectrum: Allows modeling of multiple spectral peaks in complex waters.

#### *3.1.1.10-Simulation 10*

-Wind Speed: 12 m/s, represents an intense storm, infrequent but possible in Bari.

-Horizontal Direction: 330°, wind from the north-northwest, typical at the end of a Bora storm.

-Significant Wave Height: 2.5 m, maximum simulated waves, used for resistance tests.

-JONSWAP Spectrum: Ideal for simulating storm conditions.

#### *3.1.1.11-Simulation 11*

-Wind Speed: 3 m/s, a gentle breeze, common on calm days.



- Horizontal Direction: 30°, wind from the northeast with light currents.
- Significant Wave Height: 0.5 m, low waves, typical of stable conditions.
- ISSC Spectrum: Simplified and suitable for calm waters.

#### *3.1.1.12-Simulation 12*

- Wind Speed: 9 m/s, represents a strong and sustained wind.
- Horizontal Direction: 120°, wind from the southeast, typical of Scirocco winds.
- Significant Wave Height: 1.8 m, high waves generated by moderate storms.
- TORSETHAUGEN Spectrum: Useful for modeling the interaction between local and remote waves.

#### *3.1.1.13-Simulation 13*

- Wind Speed: 11 m/s, represents an extreme condition to evaluate system stability.
- Horizontal Direction: 270° (West), waves generated in adverse conditions.
- Significant Wave Height: 2.2 m, significant waves with high energy.
- JONSWAP Spectrum: Suitable for storms in semi-enclosed seas.

### 3.1.2-RESULTS

Once the simulations for scenarios 1-13 have been carried out, studying how the wind turbine performs under these specific conditions over 60 seconds, we can carefully analyze the information deduced from the various graphs mentioned below:

- Aerodynamic Power (Illustration 37)
- Torque Coefficient (Illustration 38)
- Power Production (kWh) (Illustration 39)

It is important to note that these simulations combine different wind speeds and directions along with varying wave conditions, so the results obtained will generally show low efficiency outcomes.

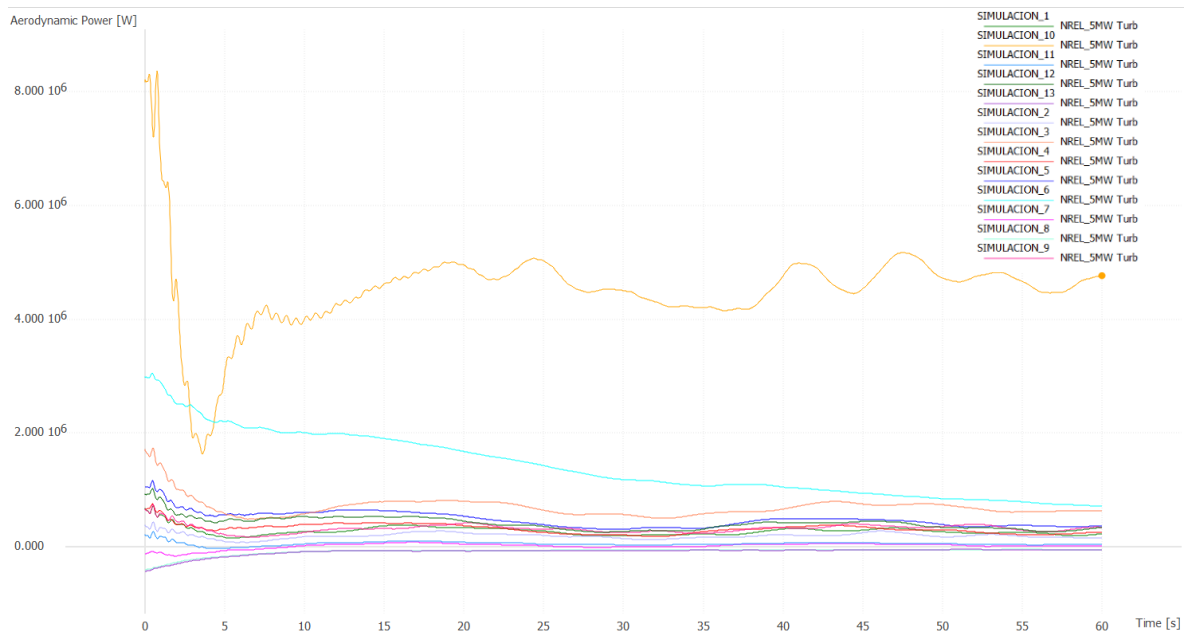


*Illustration 37-Aerodynamic Power in the different simulations (W)*

In this graph, the evolution of aerodynamic power generated by the wind turbine over the 60 seconds duration of the simulation for each of the studied scenarios is shown. It can be observed that in all cases there is an initial peak (positive or negative) followed by stabilization.

It can be deduced that the initial peak corresponds to the transient phase at the beginning of the simulation, during which the rotor is reaching a steady-state operating regime. Subsequently, aerodynamic power stabilizes, indicating that the wind turbine is working in a steady-state condition due to the constant wind speed of the simulation. However, small fluctuations in aerodynamic power are observed throughout all curves, which is

due to the inclusion of wave conditions in all scenarios, so that the wind turbine is not operating under perfectly stable conditions.

Additionally, it can be observed that with the exception of 4 curves, the other ones display similar behaviors. Below, the curves with different behaviors are identified and explained:

-Simulation 10: As can be seen in the curve corresponding to Simulation 10, aerodynamic power stabilizes around values of 5 MW, which coincides with the nominal power of the wind turbine used. This may be due to the fact that this simulation considers a wind speed of 12 m/s, very close to the turbine nominal wind speed.

-Simulations 7, 8, and 13: In these three simulations, the aerodynamic power produced is negative. From this, it can be deduced that the proposed conditions are entirely unfavorable for the wind turbine operation, and therefore, under these meteorological conditions, the wind turbine should not be operating and consequently will not produce any power.

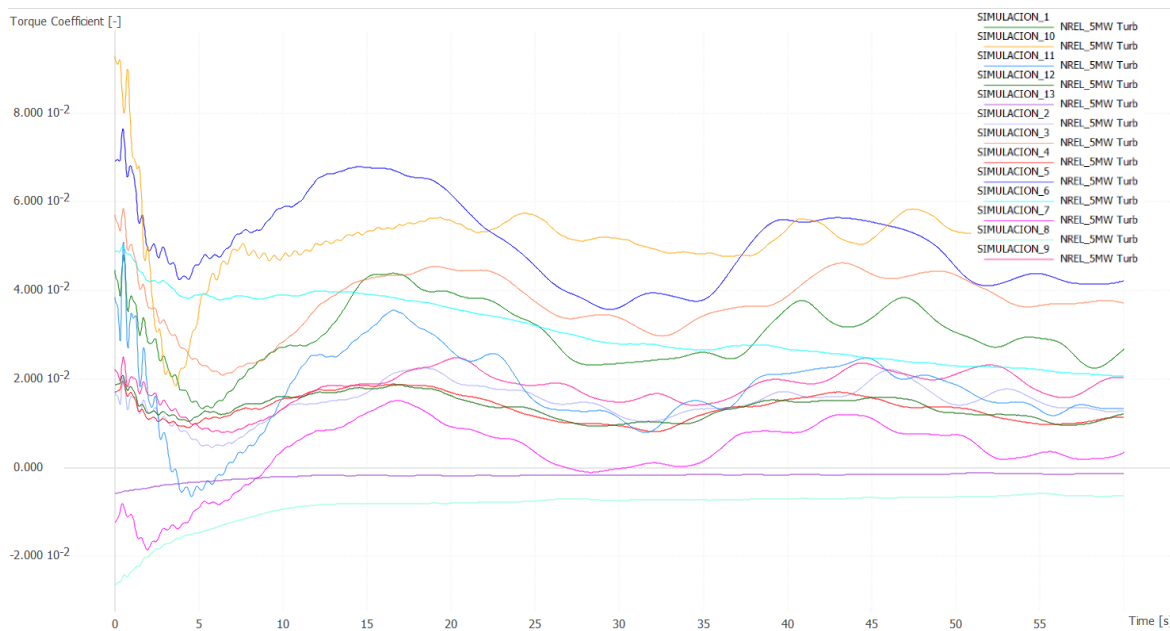


*Illustration 38- Torque Coefficient in the defined simulations*

This graph shows the evolution of the torque coefficient for each simulation over time. As in the previous graph, it can be observed that the curves stabilize over time, converging towards a steady-state regime.

As we can see, the highest values of the torque coefficient correspond to the simulations with higher wind speeds. For cases 7, 8, and 13, negative values of the torque coefficient are obtained, which justifies the previous observation that in these cases, the wind turbine will not be operational.

The stabilized values of the torque coefficient are directly related to the wind turbine ability to convert wind energy into mechanical energy.

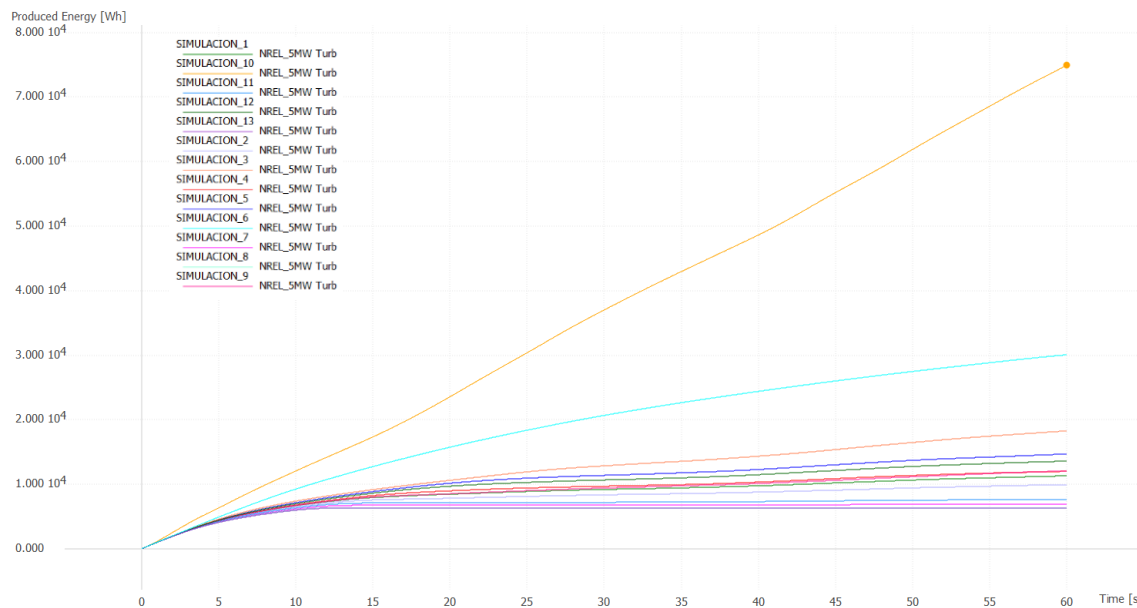


*Illustration 39-Produced energy for the defined simulations*

This graph illustrates the accumulated energy produced by the wind turbine during the simulation period. As with the previous graphs, different curves are shown for each simulation.

Like the first graph, it can be observed that the curve from Simulation 10 shows a much higher energy production than the rest of the simulations. It is also worth noting that the curves for simulations 7, 8, and 13 should not be considered for the reasons explained earlier.

Thanks to all these simulations, we can understand the different behaviors of the wind turbine under various scenarios. With a thorough study of the different climatic conditions of Bari, it could be possible to determine the wind turbine production on a given day, considering that each day the wind turbine will face different scenarios due to the large number of possible combinations of wind and wave conditions. These possible combinations make it very complex to conduct such a study for a single day, so estimating the annual production would be even more difficult.

## 3.2-ANNUAL ENERGY PRODUCTION (AEP)

The AEP (Annual Energy Production) is a key measure in evaluating the performance of a wind turbine or wind farm. It represents the total amount of electrical energy that a wind turbine is expected to generate in one year under certain wind conditions. This value is

critical for the design, economic feasibility, and planning of wind projects, as it allows for estimating the profitability and energy impact of a wind turbine.

Due to the complexity mentioned earlier about calculating the AEP of the wind turbine by considering both wind and wave conditions, a simplified calculation is chosen, using only wind speeds.

The calculation of AEP is given by the following formula:

$$AEP = \sum_{i=1}^n P(V_i) \times f(V_i) \times 8760$$

Where:

- $P(V_i)$  is the power generated by the wind turbine at wind speed  $V_i$ .

- $f(V_i)$  is the probability of the wind speed  $V_i$ .

-8760 is the number of hours in a year.

To obtain the probability of wind speeds, it is necessary to estimate the Weibull distribution, which is characterized by two parameters:

-Shape parameter ( $k$ ): Indicates the dispersion of wind speeds.

-Scale parameter ( $c$ ): Represents a measure of wind speed.

To generate the Weibull distribution applied to Bari and use it for the AEP estimation, we need an approximation of the wind speed values for Bari. According to available general data from sources like Windfinder, Bari has an average wind speed of around 5 m/s. Based on this information, we proceed to calculate the parameters and the Weibull distribution.

-Average wind speed: 5 m/s

-Shape parameter ( $k$ ): 2 (a typical approximation for areas with moderate winds)

-Scale parameter ( $c$ ): It is calculated as  $c = \frac{v_{mean}}{\Gamma(1+\frac{1}{k})}$ , by substituting the average wind speed and the shape parameter, we obtain that  $c=5.642$  m/s, approximately 5.64.

In the next image (Illustration 40), a graph is shown where the Weibull distribution to be used for annual production estimation is represented.

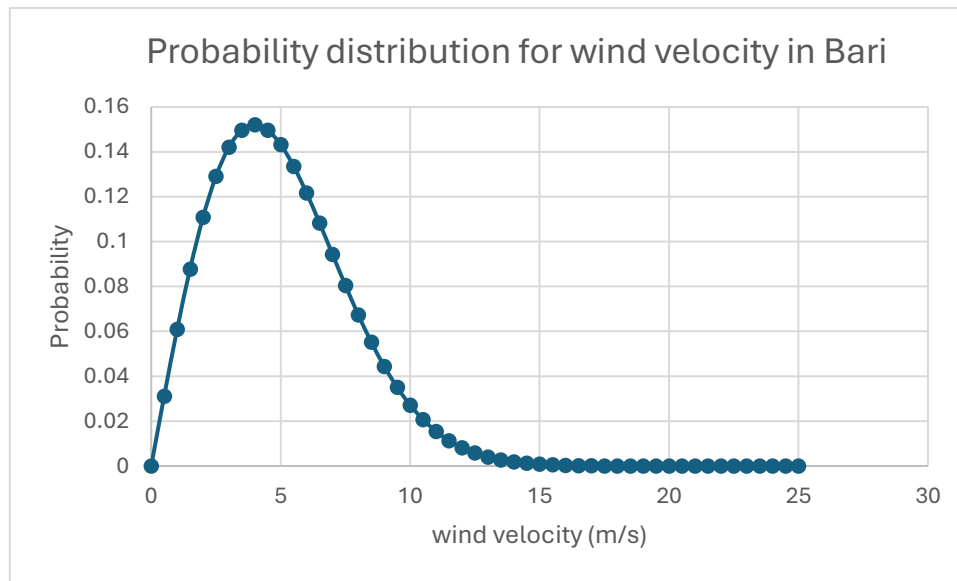


*Illustration 40-Weibull distribution for wind velocity in Bari  $K=2$ ,  $c=5,64$  and  $v_{med}=5\text{m/s}$*

To generate this graph, the Weibull probability density function is used, which is calculated as:

$$f(v) = \left(\frac{k}{c}\right) \left(\frac{v}{c}\right)^{k-1} e^{-\left(\frac{v}{c}\right)^k}$$

Once the Weibull distribution is estimated, the next step is to calculate the power generated by the wind turbine. To do this, we need to consider that the turbine with which we are working typically operates with a TSR of 7.55 between the cut-in wind speed (3 m/s) and the nominal wind speed (11.4 m/s). After the nominal wind speed (at which the nominal power is achieved), the wind turbine operates at this nominal power until the wind speed reaches 25 m/s, at which point the wind turbine shuts down to prevent damage. Therefore, if we perform a multi-BEM analysis in the QBlade application, we can establish the power curve for the turbine operating conditions.

To obtain this power curve, the first thing to calculate is the rotational speed of the rotor based on the wind speed. Given the TSR and the wind speed, we can apply the following formula:

$$\omega = \frac{TSR \times v}{R} \times \frac{60}{2\pi}$$

In the next image (Illustration 41), the results obtained can be observed.

velocidad m/s	0.00	1.00	2.00	3.00	4.00	5.00	6.00	7.00	8.00	9.00	10.00	11.00
rpm	0.00	1.14	2.29	3.43	4.58	5.72	6.87	8.01	9.16	10.30	11.44	12.59

*Illustration 41-Wind and rotor velocity for constant  $TSR=7,55$*

As long as these operating conditions are met, the wind turbine will be operating under optimal conditions. Therefore, if we return to QBlade and perform a multi-BEM analysis, we can construct the power curve.

Once the simulation is complete, the following result is obtained (Illustration 42).

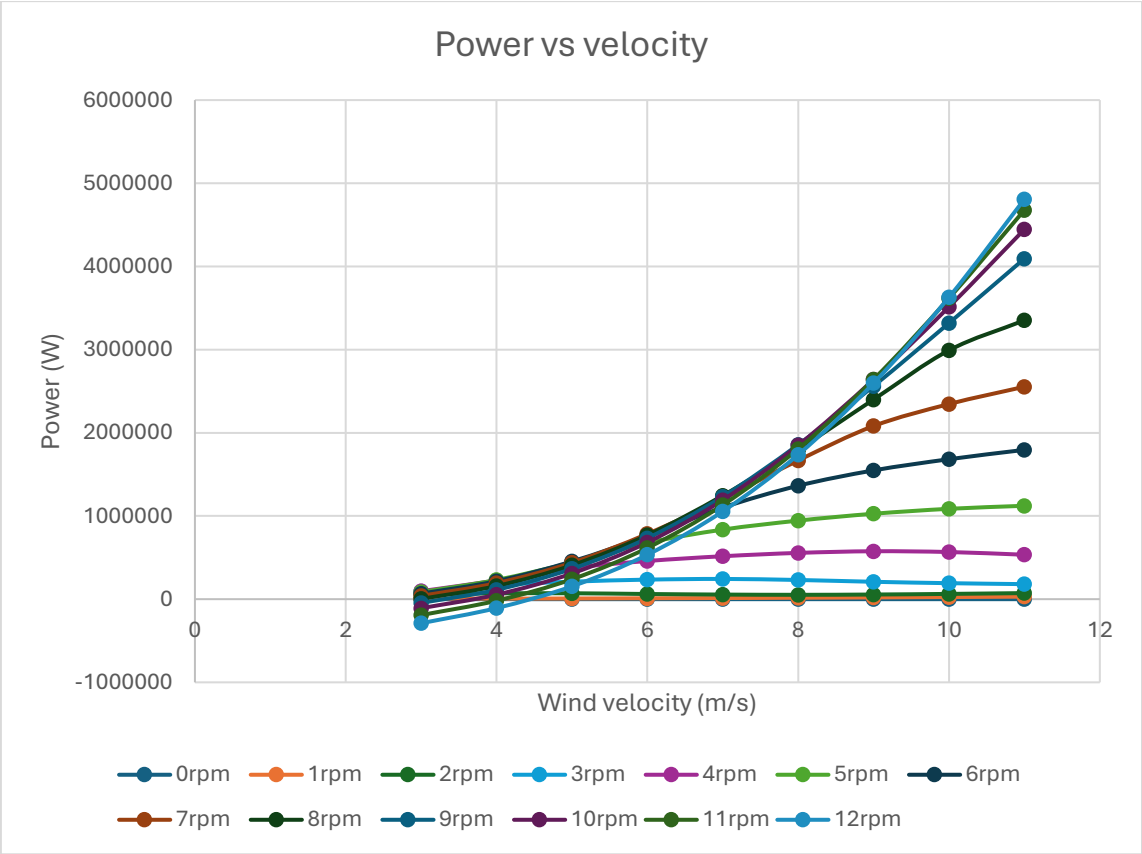


*Illustration 42-Power vs velocity obtained with multi-BEM analysis*

In this graph, constructed from the simulation data, the power curve for a constant TSR can be determined. The graph shows the power generated for each wind speed, depending on the rotor speed (each curve in a different color). By using this graph, we can construct the first part of the power curve between the cut-in speed and the nominal speed. To do this, one could use this graph (multi-BEM analysis for large intervals) to obtain approximate values, or alternatively, export the data to an Excel file by running a simulation (multi-BEM analysis for very small intervals) and build the curve with the specific data for each wind and rotational speed.

We have chosen the most precise results. The graphs obtained and the tables exported to Excel are not shown as they take up too much space and are very complex to view. The results we obtained are shown in the following table (Illustration 43).

velocity (m/s)	rpm if TSR=7.55	Power (kW)
3	3.43	97.98
3.5	4.01	155.68
4	4.58	232.47
4.5	5.15	331.05
5	5.72	453.82
5.5	6.29	604.207
6	6.87	784.58
6.5	7.44	996.95
7	8.01	1245.48
7.5	8.587	1532.7
8	9.16	1859.74
8.5	9.73	2229.76
9	10.29	2647.30
9.5	10.87	3113.92
10	11.44	3630.55
10.5	12.02	4203.48
11	12.59	4833.66
11.5	13.16	5382.59

Illustration 43-Power generated

Once all the power data is stored, the graph can be constructed making the considerations mentioned earlier. That is a graph divided into two sections (constant TSR and constant power) will be obtained. It can be seen in the following image (Illustration 44).

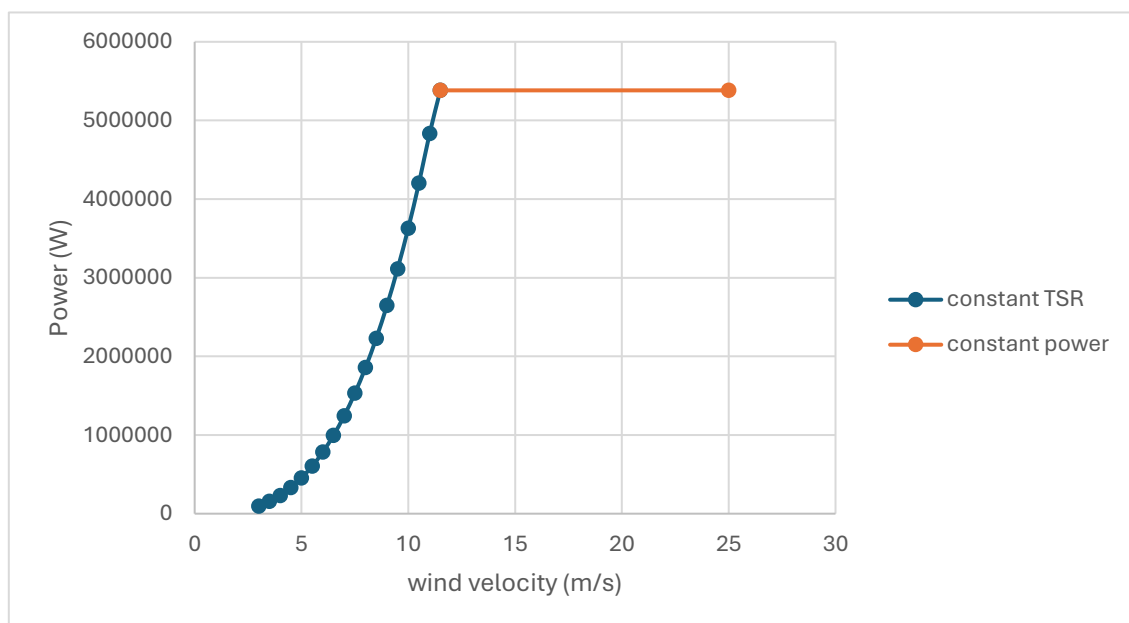


Illustration 44- Power graph for the NREL 5MW



Once obtained the Weibull distribution and the power curve, the AEP (Annual Energy Production) can be calculated using the formula:

$$AEP = \sum_{i=1}^n P(V_i) \times f(V_i) \times 8760$$

For each velocity it is obtained the following results (illustrations 45 y 46)

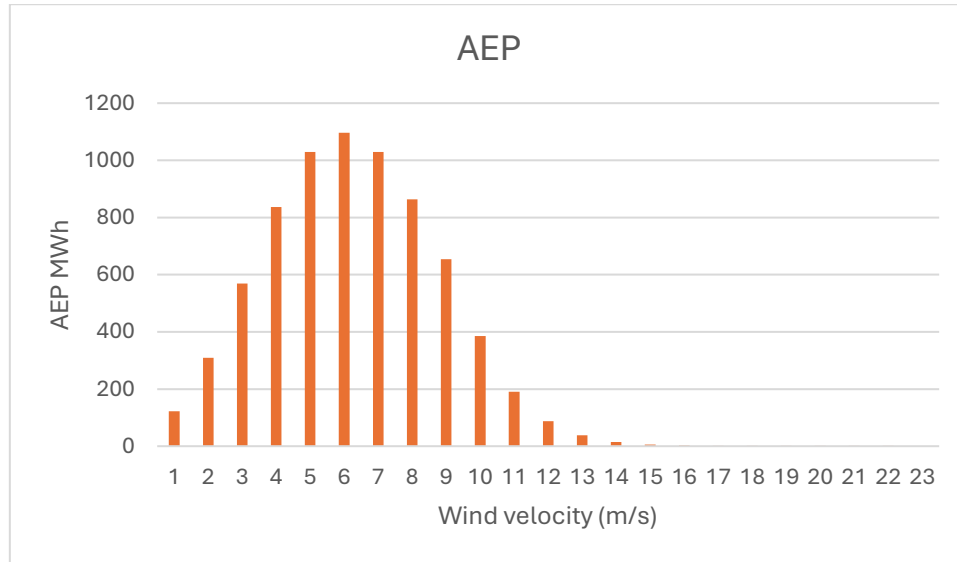


Illustration 45-AEP for NREL 5MW

velocity (m/s)	P(vi)	f(vi)	AEP (MWh)
3	97983.24	0.1421	121.94
4	232467.34	0.1520	309.59
5	453819.28	0.1432	569.42
6	784577.31	0.1216	836.17
7	1245475.5	0.0943	1029.39
8	1859738.8	0.0673	1096.58
9	2647304	0.0443	1029.46
10	3630554.3	0.0271	863.60
11	4833656	0.0154	653.88
12	5382594	0.0081	385.66
13	5382594	0.0040	190.49
14	5382594	0.0018	87.84
15	5382594	0.0008	37.84
16	5382594	0.0003	15.24
17	5382594	0.0001	5.74
18	5382594	4.295E-05	2.02
19	5382594	1.418E-05	0.6686
20	5382594	4.384E-06	0.2067
21	5382594	1.269E-06	0.0598
22	5382594	3.445E-07	0.0162
23	5382594	8.762E-08	0.0041
24	5382594	2.088E-08	0.0009
25	5382594	4.667E-09	0.0002

Illustration 46-AEP for NREL 5MW

Through this graph of annual production, several data points can be deduced. The first and most important is that the sum of everything provides an estimate of how many MWh the wind turbine will produce in the Bari region.

As a consequence of the Weibull distribution for this area, we can also see that the generator will produce more energy when operating at lower wind speeds (5, 6, and 7 m/s) than at higher speeds.

In total, if the NREL 5MW is installed in the Bari region, it will produce approximately 7235.89 MWh.

To estimate the average annual electricity consumption of a household in Italy, macroeconomic data can be considered. In 2022, Italy's total electricity consumption was 298,320 GWh, with a per capita consumption of approximately 5,056.5 kWh.

Given that the average size of Italian households is around 2.3 people, it can be estimated that the average annual electricity consumption per household is approximately 11,630 kWh. This leads to the conclusion that the wind turbine could generate enough energy to supply around 622 households.

Translating the production to an economic impact, considering that according to the macro data (June 2024), the latest recorded electricity price is 327.4 €/MWh, we can calculate that a wind turbine will produce the equivalent of 2.37 million euros.

## 6-CONCLUSION

This work has yielded important information.

First, we have learned some of the most basic concepts and knowledge about the importance and operation of wind turbines. This understanding highlights the critical role that the development of renewable energy plays as an alternative to polluting energy sources.

Additionally, we have become familiar with a wind turbine simulation program, Qblade, which offers a wide range of possibilities for studying wind turbine performance. We learned how to use each of the modules in the program, and thanks to it, we were able to assess the project of an existing wind turbine, the NREL 5MW OC4 Semisub.

By analyzing the results obtained from the simulations, we gained insight into the complexity of studying the energy production of a wind turbine when combining wind and wave scenarios. As a simplification, we conducted a study on the annual production of wind turbines in the Bari region, considering only wind data.

The results obtained were promising, showing that a single wind turbine is capable of supplying over 600 households annually and generating the equivalent of over two million euros. It is true that this wind turbine could supply many more households, as the region of Bari experiences moderate winds with a Weibull distribution centered around 5 m/s. However, the wind turbine we worked with is designed to operate at 11.4 m/s. Therefore, we can conclude that the NREL 5MW model would be more effective in other regions with higher average wind speeds.

## 7-REFERENCES

- Robertson, A., Jonkman, J., Masciola, M., Song, H., Goupee, A., Coulling, A., & Luan, C. (2014). *Definition of the Semisubmersible Floating System for Phase II of OC4* (Technical Report No. NREL/TP-5000-60601). National Renewable Energy Laboratory.
- Noticias CEA. (s.f.). ¿En qué se diferencian los parques eólicos terrestres de los marítimos?
- Burton, T., Sharpe, D., Jenkins, N., & Bossanyi, E. (2011). *Wind energy handbook*. John Wiley & Sons.
- Fischer, K., Schaumann, P., & Thiele, K. (2010). Corrosion protection for offshore wind turbines. *Wind Engineering*, 34(3), 251-266.
- Jonkman, J. M., Butterfield, S., Musial, W., & Scott, G. (2009). Definition of a 5-MW reference wind turbine for offshore system development. *National Renewable Energy Laboratory*.
- Molins, C., Campos, A., & Casals, O. (2014). Analysis of floating offshore wind turbines subjected to moderate waves. *Ocean Engineering*, 88, 294-305.
- Open-Source Physics. (s.f.). *QBlade User Manual: Wind Turbine Design and Simulation Software*.
- National Renewable Energy Laboratory (NREL). (2009). *Definition of a 5-MW Reference Wind Turbine for Offshore System Development*.
- National Renewable Energy Laboratory (NREL). (2014). *OC4 Phase I: Final Definition of the Floating Offshore Wind Turbine Platform*.
- International Energy Agency (IEA). (2021). *Offshore Wind Outlook 2021*.
- Open Source Physics. (s.f.). *QBlade: Wind Turbine Design and Simulation Software*.
- Global Wind Energy Council (GWEC). (2023). *Global Wind Report 2023*.
- Viterna, L. A., & Corrigan, R. D. (1981). Development of a High Lift Airfoil for Large Horizontal Axis Wind Turbines. NASA Technical Paper 2005, NASA Lewis Research Center.
- Montgomery, J. S., & Leung, K. C. (1989). Wind Turbine Aerodynamics and Design Considerations. Proceedings of the Wind Energy Symposium.
- Ledoux, J., Rizzo, S., & Salomon, J. (2020). *Analysis of the Blade Element Momentum Theory*. Retrieved from <https://arxiv.org/abs/2004.11100>

Ning, A. (2020). *Using Blade Element Momentum Methods with Gradient-Based Design Optimization*. Retrieved from <https://flowlab.groups.et.byu.net/preprints/Ning2020.pdf>

QBlade Documentation. *Blade Element Momentum Method*. Retrieved from <https://docs.qblade.org/src/theory/aerodynamics/bem/bem.html>

Copernicus Climate Change Service (C3S). (n.d.). ERA5: Fifth generation of ECMWF atmospheric reanalyses of the global climate.

ECMWF (European Centre for Medium-Range Weather Forecasts). (n.d.). ECMWF Reanalysis Datasets.

World Meteorological Organization (WMO). (n.d.). Guide to Wave Analysis and Forecasting. Retrieved from [https://library.wmo.int/doc\\_num.php?explnum\\_id=3811](https://library.wmo.int/doc_num.php?explnum_id=3811)

Holthuijsen, L. H. (2007). *Waves in Oceanic and Coastal Waters*. Cambridge University Press.

MedGLOSS Project. (n.d.). Mediterranean Sea wave data and forecasts. Retrieved from <http://medgloss.ocean.org.il>

Datosmacro. (n.d.). *Consumo eléctrico en Italia*. Expansión. Recuperado el 14 de enero de 2025, de <https://datosmacro.expansion.com/energia-y-medio-ambiente/electricidad-consumo/italia>

Datosmacro. (2024). *Italia - Precios de la electricidad de los hogares*. Recuperado de [Datos Macro](#)

## 8-APPENDICES

Illustration 1-wind turbines .....	5
Illustration 2-HAWT and VAWT .....	7
Illustration 3-Fixed-Botton wind turbines .....	8
Illustration 4-Floating wind turbines.....	9
Illustration 5-NREL 5MW OC4 SEMISUB model.....	10
Illustration 6-Floating platform.....	11
Illustration 7-Features of the floating platform .....	11
Illustration 8-Table of airfoil generator.....	16
Illustration 9- Airfoils profiles from NREL 5MW.....	17
Illustration 10-Analysis results.....	18
Illustration 11- Graph of the lift-to-drag ratio versus the angle of attack.....	19
Illustration 12- Graph of the drag coefficient versus the angle of attack .....	20
Illustration 13- Graph of pressure distribution along the DU21_A17 aerodynamic profile when $\alpha=-10^\circ$ .....	21
Illustration 14- Graph of the boundary layer .....	22
Illustration 15- Results of the polar extraplation.....	23
Illustration 16-Manual blade design option .....	25
Illustration 17-Blade characteristics.....	26
Illustration 18 – NREL 5MW blades design .....	27
Illustration 19- First mode .....	28
Illustration 20-Second mode .....	28
Illustration 21-Third mode... ..	28
Illustration 22-Fourth mode.....	28
Illustration 23-BEM Analysis for NREL 5MW at 10m/s .....	30
Illustration 24- Graph of Power Coefficient ( $C_p$ ) versus Tip Speed Ratio .....	31
Illustration 25- Graph of Thrust Coefficient ( $C_t$ ) versus Tip Speed Ratio .....	32
Illustration 26- Graph of Angle of Attack versus Radius .....	32
Illustration 27- Graph of Axial Induction Factor versus Radius .....	33
Illustration 28-Load case when $TSR=1$ .....	34
Illustration 29-Load case when $TSR=12$ .....	35
Illustration 30-Window for turbine and structure modeling .....	36
Illustration 31-NREL 5MW OC4 Semisub model.....	37
Illustration 32-Simulation window .....	38
Illustration 33-Wave generator window .....	39
Illustration 34-Wave spectrum generated.....	40

Illustration 35-Wind conditions table.....	41
Illustration 36-Wave conditions table.....	42
Illustration 37-Aerodynamic Power in the different simulations (W) .....	46
Illustration 38- Torque Coefficient in the defined simulations.....	47
Illustration 39-Produced energy for the defined simulations .....	48
Illustration 40-Weibull distribution for wind velocity in Bari $K=2$ , $c=5,64$ and $v_{med}=5\text{m/s}$ .....	50
Illustration 41-Wind and rotor velocity for constant $TSR=7,55$ .....	50
Illustration 42-Power vs velocity obtained with multi-BEM analysis .....	51
Illustration 43-Power generated .....	52
Illustration 44- Power graph for the NREL 5MW.....	52
Illustration 45-AEP for NREL 5MW .....	53
Illustration 46-AEP for NREL 5MW .....	53